ARCHIVES OF ALLIED HEALTH SCIENCES

Archives of ALLIED HEALTH SCIENCES

Arch AHS
Volume 35
Issue 3
2023

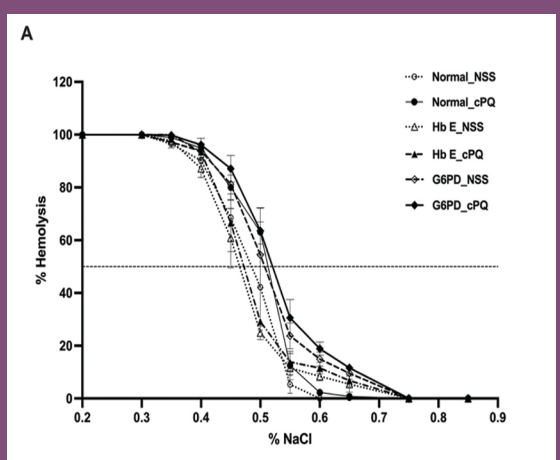

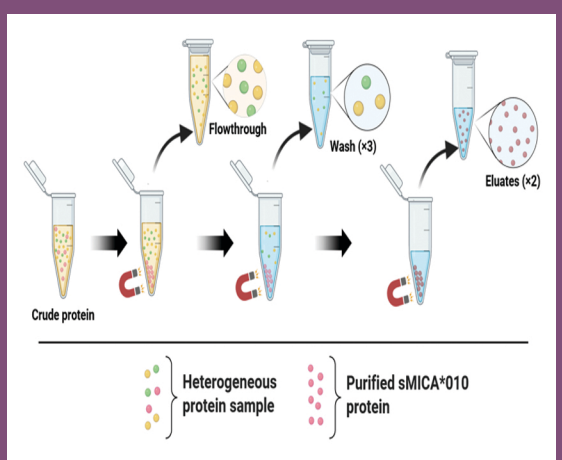

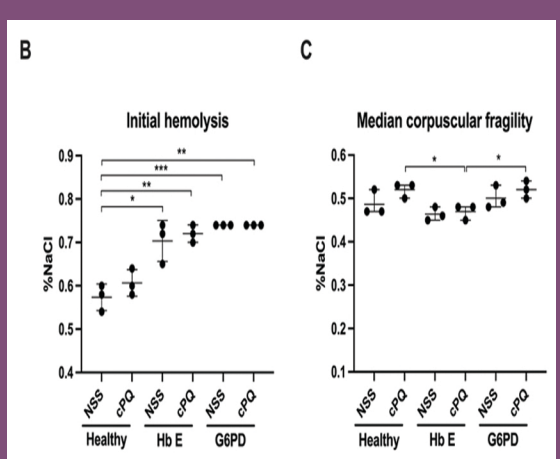

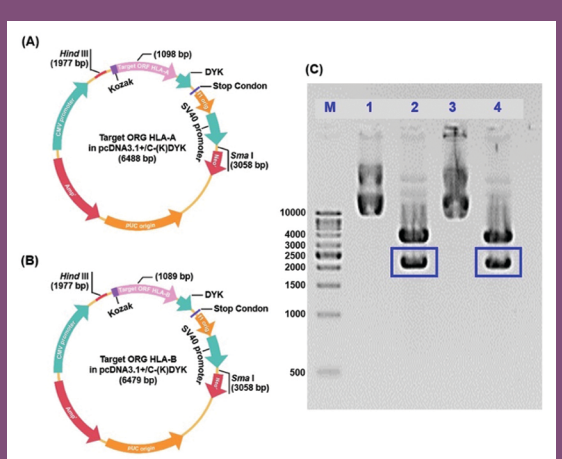

ISSN 2730-2008 (Online)

https://www.tci-thaijo.org/index.php/ams

Volume 35, Issue 3, 2023

Arch AHS

ARCHIVES OF ALLIED HEALTH SCIENCES

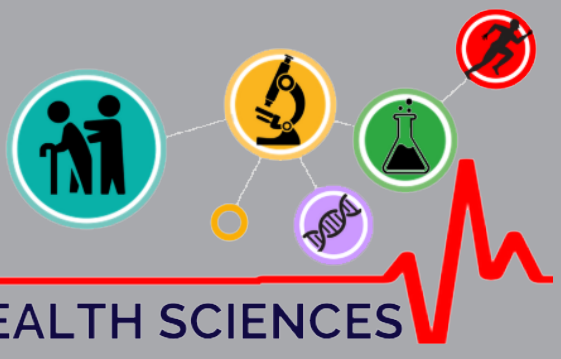

The **Archives of Allied Health Sciences (Arch AHS)** is an international peer-review multi-disciplinary journal published in English. It is owned by the Faculty of Associated Medical Sciences, Khon Kaen University, Thailand. The Arch AHS was formally known as *Journal of Medical Technology and Physical Therapy (JMTPT)*, which was founded in 1989. The title of the journal was changed to ***the Archives of Allied Health Sciences (Arch AHS)*** from 2020 (volume 32 issue 2: May - August) onward.

The Arch AHS aims to be a leading forum for research and knowledge in evidence-based practice relating to Allied Health Sciences. Contributions from all parts of the world and from different professionals in Allied Health Sciences are encouraged. Original articles, reviews, special reports, short communications, and letters to the editor are published 3 regular issues per year, online and in print.

Production and editorial assistance:
Arpassanan Wiyanad
Roongnapa Intaruk

All correspondence concerning manuscripts, editorial issues and subscription should be addressed to:
Editorial Officer: ArchAHS.TH@gmail.com
Faculty of Associated Medical Sciences,
Khon Kaen University, Thailand.

Publication information:
Arch AHS (ISSN: 2730-1990; eISSN: 2730-2008)
appears 3 issues a year.
Issue 1 January – April;
Issue 2 May – August;
Issue 3 September – December.

Indexing:
Arch AHS is indexed in Thai Citation Index (TCI tier 1) and ASEAN Citation Index (ACI) databases.

Manuscript preparation:
Please review author guideline for manuscript preparation: https://drive.google.com/drive/folders/1kO5FijEnuLSYwzgKcnQ9mxO74ZZ0wGRA

Link to website

Arch AHS
ARCHIVES OF ALLIED HEALTH SCIENCES

Contents

ORIGINAL ARTICLE

Arch AHS

Archives of Allied Health Sciences 2023; 35(3): 1-10.

Gross motor and language developmental stimulation via play during sitting attainment in orphaned infants

Sunanta Prommin[1], Surussawadi Bennett[1], Ponlapat Yonglitthipagon[2], Lugkana Mato[2], Michael John Bennett[3,4], Wantana Siritaratiwat[1*]

[1] Research Center in Back, Neck, Other Joint Pain and Human Performance (BNOJPH), Faculty of Associated Medical Sciences, Khon Kaen University, Khon Kaen, Thailand.

[2] School of Physical Therapy, Faculty of Associated Medical Sciences, Khon Kaen University, Khon Kaen, Thailand.

[3] University Hospital Southampton NHS Foundation Trust, Southampton, United Kingdom.

[4] Faculty of Medicine, University of Southampton, Southampton, United Kingdom.

KEYWORDS

Independent sitting; Orphaned infants; Alberta Infant Motor Scale; Language development; Gross motor development.

ABSTRACT

Orphaned infants often show delayed language development due to their limited child-rearing practices. The stimulation of language development before the attainment of sitting is questionable. The aim was to compare the scores of language and gross motor development before and after one-month stimulation program. Two groups of 20 healthy full-term orphaned infants aged 6-9 months were recruited for this quasi-experimental study. The first group consisted of infants who sat with support, and the second group consisted of those who sat independently. All infants received routine care and a program of substitutional 45-minute structured play three days per week for four weeks. The gross motor development of infants was directly observed using the Alberta Infant Motor Scale, and language development was assessed using the Communication and Symbolic Behaviors Scales-Developmental Profile Infant-Toddler Checklist at the pre- and post-four-week stimulation program. The differences in outcomes before and after intervention were examined using the paired t-test and the Wilcoxon signed-rank test. There were no significant differences in the means of language scores before and after four-week stimulation programs in both groups of infants, while both groups exhibited significant differences in gross motor development. Therefore, the stimulation program via play while attaining sitting skills may enhance language development in orphaned infants.

***Corresponding author:** Wantana Siritaratiwat, PT, PhD. Research Center in Back, Neck, Other Joint Pain and Human Performance (BNOJPH), Faculty of Associated Medical Sciences, Khon Kaen University, Khon Kaen, Thailand. Email address: wantana@kku.ac.th

Received: 27 May 2023/ Revised: 8 July 2023/ Accepted: 18 July 2023

Introduction

Orphaned infants, compared to home-raised infants, are not exposed to diverse nurturing environments. As a consequence of the caretakers' high workload and the child-rearing environment in orphanages, child care institutions appear limited in infants' daily activity and human interaction. Infants in orphanages are frequently raised in confined spaces or spend most of their time in cots due to insufficient caregivers and precautions put in place to prevent potential accidents among infants. Infants in this environment are prone to having little chance of contact with diverse movement experiences or to interact with various objects in daily living. A previous longitudinal study demonstrated that orphanage-raised 6-9-month-old infants displayed narrow intra-individual variability in gross motor development[1]. These orphaned infants also showed their gross motor percentiles below the 50th percentile via series assessments[1,2]. Several pieces of evidence also indicated that infants raised in orphanages exhibited delayed development in at least one domain, such as gross motor or language development[3-5]. Previous cross-sectional studies reported deficits in gross motor skills[3,4], especially sitting and standing, languages[3], and cognitive development[5] in orphanage-raised infants.

The acquisition of gross motor skills, such as sitting, crawling, and pulling to stand, is clearly noticeable between the ages of six and nine months in healthy, typically developing infants. An independent sitting ability, in which infants can control the head and various segments of the trunk[6,7], is a crucial developmental milestone. According to a WHO multicenter study, typically developing infants exhibit an ability to sit without support within a wide range of age before the first year of life[8]. In addition, the ability to sit also enables infants to perform independent reaching and interact with objects around them[9].

In relation to objects and child-rearing contexts during the second half of the first year of gross motor skill acquisition, infants develop a basis of language acquisition and communication abilities[10]. Previous studies have shown that language and motor skills are closely interrelated in development. There are correlations between gross motor skills, especially sitting[7,11], and language development in healthy typically developing infants. Libertus and Violi[7] found that the emergence of sitting skills is a significant predictor of subsequent language development in healthy developing infants. The cross-sectional studies found correlations between gross motor skills and language development in infants aged between three months and three years[12,13]. It has been suggested that motor scores were significantly related to receptive, expressive vocabulary or language development when oral movement, gross motor score, gesture, and symbolic function are taken into account. In addition, infant receptive and productive vocabularies were increased when they were exposed to functional locomotor activity[14]. Infants in the age of learning to sit also demonstrate chattering, which is a part of language development[15]. Typically developing infants also showed a significant relationship between motor and language development, as early as 6 to 12 months. The ability to lift the chest with arm support at six months was found to be positively correlated with turning toward sound[16].

The beginning of language development stimulation in children with delayed language development clinically starts when they are able to sit independently. Given the significant relationship between gross motor and language development, language skills could be simultaneously developed at around the age of sitting attainment[12,13,16]. The stimulation of language development in orphaned infants when infants are still sitting with support is a topic of interest in the current study. Our study questioned whether language development could be improved

through play programs administered to infants who sat with support[15,16]. Furthermore, data regarding developmental stimulation in language development in orphaned infants, particularly during the period of sitting skill acquisition, is limited. We hypothesized that through one-month structured play during sitting attainment, healthy orphaned infants would exhibit enhanced language and gross motor development. The reason why a four-week period was chosen to measure the outcomes after intervention, as it is enough to observe changes in gross motor development[17], nevertheless, there was no data supporting the amount of time needed for language stimulation in young orphaned infants. Therefore, this study aimed to compare the scores of language and gross motor development of healthy orphaned infants before and after a four-week stimulation program. Comparisons between pre- and post-intervention were performed in two groups of infants: those who sat with support and those who sat independently.

Materials and methods

Study design and description of the orphanage setting

The current quasi-experimental study was conducted in healthy full-term orphanage-raised infants. Routine care was provided by caregivers with more than 10 years of experience in orphanage care for infants aged from birth to one year. Infants live in one room located in a two-story building. The ratio of caregivers to infants is 1 caregiver to 7–10 infants. All caregivers are female, with an average age of 45 years. The routine stimulating care consists of a five-minute massage session after a morning bath and free play on the floor for 45 minutes, once or twice each day on weekdays, depending on the availability of caregivers. In addition to bottle feeding, infants receive regular baths once or twice a day, diaper changes as needed, and meal feedings at lunch and dinner.

Participants

From a registry of orphaned infants, 6- to 9-month-old healthy infants with a gestational age of more than 37 weeks were conveniently recruited. Infants were excluded if they presented with the following criteria: 1) major neurological abnormalities, such as muscle paralysis, jerky movements, and seizures; 2) genetic diseases, such as Down's syndrome; 3) congenital diseases, such as heart disease and musculoskeletal disorders; and 4) deficits in vision or hearing, as well as issues affecting motor development. The first group contained infants who sat with support, and the second group had those who sat independently. In this study, the definition of "sat independently" was defined as infants demonstrating a sitting posture and achieving the score on the sitting picture of item no. 9 of the Alberta Infant Motor Scale (AIMS)[18]. This is observed as an infant in a sitting posture displaying the act of reaching for a toy and trunk rotation with ease. While infants who sat with support means those who cannot sit by themselves or could not attain the score on the sitting picture of item no. 9 of the AIMS[18].

Ethical clearance

The study protocol was approved by the Ethics Committee in Human Research at Khon Kaen University based on the Declaration of Helsinki and the ICH Good Clinical Practice Guideline (Institutional Review Board Number: IRB00008614, Protocol ID No: HE622234, 04/12/2019). The guardian of the orphanage signed an informed consent form authorizing data collection at the orphanage and the voluntary participation of staff and infants. Data collection occurred between December 2019 and September 2021. The researcher scheduled data collection visits after the head of the orphanage and staff had given their informed consent to participate voluntarily and to allow their infants to be assessed for gross motor and language development. The data were anonymized so as not to disclose the identities of the participants,

and the analyses were conducted so that the final results could not be traced back to specific individuals.

Experimental procedure

The following participant characteristics were recorded: gender, birth weight, birth height, head circumference, gestational age, Apgar score at five minutes, and age upon admission to the orphanage. Infants were initially recruited between the ages of six and nine months, and the first data collection commenced 15 days after recruitment. Each infant was assessed twice, prior to and after a post-one-month intervention.

Interventions

A 45-minute structured play for infants who sat with support

Infants received a substitutional program of 45-minute structured play, which was modified from a previous study[19], three days per week for four weeks by pediatric physiotherapists who had over five years of expertise working with orphaned infants. The 45-minute structured program included a 30-minute play session in an upright posture and a 15-minute free-movement session on the floor. The 30-minute play consisted of 20 minutes playing with toys while sitting or standing with pelvic support and a 10-minute seated session listening to a storybook, singing a song, clapping hands, and enjoying peek-a-boo. Throughout the 15-minute period of free movement on the floor, infants were able to move in and out of various positions under supervision.

A 45-minute structured play for infants who sat independently

Infants received a substitutional program of 45-minute structured play, which was modified from a previous study[19], three days per week for four weeks by pediatric physiotherapists who had over five years of expertise working with orphaned infants. The 45-minute structured program included a 30-minute play session in an upright posture and a 15-minute free-movement session on the floor. The 30-minute play for infants was 20 minutes of actively playing with the toys while sitting or cruising and a 10-minute session of standing and walking with support outside the building once a week, or 10 minutes of listening to a storybook, singing a song, clapping hands, and enjoying peek-a-boo twice a week. Throughout the 15-minute period of free movement on the floor, infants were able to move independently in and out of various positions, such as creeping, crawling, sitting, pulling to stand, and standing under supervision.

Toys were used to encourage physical movement in these sessions. Infants joined the stimulation program only when they were feeling well and cooperated, such that they could sit with support, hold heads in the midline, or stand with support and stand on their feet or with the variable movement of legs[18]. The play activities were terminated if the infant cried or showed distress.

Outcome measures

The Communication and Symbolic Behavior Scales-Developmental Profile (CSBS-DP) Infant-Toddler Checklist

The CSBS-DP checklist is a parent- or caregiver-reported measure of infants and toddlers aged 6 to 24 months' communicative and symbolic abilities[20]. The observation can be performed on three composites of language development, including social communication, speech (sound and word use), and symbolic behaviors. The three composites contain 24 items, and each item could be scored with an ordinal scale of 0 points for "Not Yet," 1 point for "Sometimes," and 2 points for "Often." Items describing a series of numbers can be scored with 0 points for items checked "None" and 1–4 points for numbered choices. The total of CSBS-DP scale of 57 scores were added together from 26 of social scores, 14 of speech scores, and 17 of symbolic scores[20]. Raw scores of each composite and the total raw scores of language development were transferred to the standard scores using the Easy Score program (Infant–Toddler Checklist and Easy

Score©2002, Paul H. Brookes Publishing Co, Inc) [20]. Each composite contains standard scores of 17, and the total standard scores are 135.

The main primary caregiver, who was familiar with infants, performed a checklist of the early communication and behavioral development of each participant using the CSBS-DP[20]. The primary caregiver completed the behavioral checklist for each infant within 10 minutes. If the infant did not cooperate or other factors interfered, the assessor performed the test again within five days of the initial assessment. The therapist also monitored each child to eliminate over- or underestimation of the infants' language ability. The main caregiver was unaware of how each observation and checklist was scored. All tests' scoring was performed and double-checked by pediatric physical therapists.

Alberta Infant Motor Scale (AIMS)

The AIMS is a standardized norm-referenced observation, and the performance-based test commonly utilized in research to evaluate the spontaneous movement of infants from birth until the age of independent walking attainment[18]. The test measures components of postural control, antigravity movements, and body alignments, such as trunk rotation and weight shifting in different positions, including 21 items in the prone, 9 items in the supine, 12 items in the sitting, and 16 items in the standing positions. The total raw scores range from 0 to 58[18].

The AIMS Thai version[21] was utilized to evaluate the gross motor development of each participant during the observation by a physical therapist with six years' experience in pediatric physical therapy. The assessor performed the observation in the orphanage's living room, where the infants were familiar with the environment and the main caregiver was present nearby. The observation time was approximately 20 minutes for each participant. To prevent bias, raw scores of gross motor development were totaled by another researcher and the assessor did not know the scores until data collection was completed.

The intra-rater reliability performed by the physical therapist with one-month interval showed a high intraclass correlation coefficient (ICC) value (ICC (3,1) = 0.99, 95%CI = 0.98-0.99). This assessor practiced using the AIMS for six months before data collection, and the inter-rater reliability between the assessor and the expert, with more than 10 years of using the AIMS, using the ICC (3,1) was 0.98 (95%CI = 0.95-0.99).

Statistical analysis

All participants' demographic data were characterized by descriptive statistics. The normality of the data was analyzed using a Shapiro-Wilk test. Non-normally distributed data was analyzed using the Wilcoxon signed-rank test, while normal distributed data was analyzed using the paired t-test. The levels of effect size convention were analyzed and classified as < 0.49 = small, 0.50-0.79 = medium, and ≥ 0.80 = large[22]. SPSS version 17.0 for Windows (licensed by Khon Kaen University, Khon Kaen, Thailand) was used to perform the data analyses, with a significance level of p-value < 0.05.

Results

According to the birth characteristics presented in table 1, all participants in this study were healthy, with full-term births. They had been admitted to the orphanage at a minimum age of 10 days. The mean ± SD age of infants who sat with support at recruitment was 7.1 ± 0.7 months, and their mean sitting score was 5.9 ± 2.7 points. Infants who sat independently had a mean ± SD age at recruitment of 8.2 ± 0.7 months, with a mean sitting score of 10.5 ± 2.2 of a total of 12 points. There were 12 boys in the "sat with support" group and 14 boys in the "sat independently" group.

Table 1 Participants' characteristics

Birth characteristic	Sat with support group (n = 20)	Sat independently group (n = 20)
Birth weight (g)	2717.7 ± 223.9	2756.1 ± 229.4
Birth height (cm)	49.5 ± 3.0[a]	47.8 ± 2.1[b]
Birth head circumference (cm)	31.8 ± 1.3[a]	31.6 ± 1.3[b]
Gestational age (weeks)	38.2 ± 0.6	37.8 ± 0.9
Apgar score at 5 minutes	9.1 ± 0.6[a]	9.3 ± 0.5[b]
Age at admission in the orphanage (days)	54.6 ± 43.1	79.8 ± 47.0

Note: Data was presented with mean ± SD. [a] No information on birth height, birth head circumference of 3 infants, and Apgar score of 5 infants in sitting with support group. [b] No information on birth height, birth head circumference of 3 infants, and Apgar score of 5 infants in the sat independently group.

Table 2 shows that language scores obtained from the CSBS-DP were slightly increased in both groups of participants after a four-week stimulation program. However, there were no significant differences in the mean ± SD of language scores before and after the stimulation program in both groups of infants. In analyses of the sub-composite of language development, there were no significant differences in any composite of language skills before and after the one-month intervention for both groups of infants.

Gross motor scores, obtained using AIMS, of infants in both groups differed significantly before and after the stimulation program (*p*-value = 0.001), with a large effect size: 1.01 for infants who sat independently and 1.61 for infants who sat with support. Infants in the sat with support group displayed significantly increased scores in all sub-scales of gross motor development, while infants who sat independently showed significant improvement in prone and standing sub-scales.

Table 2 Mean ± SD of the CSBS-DP and AIMS scores of infants who sat with support (n = 20) and those who sat independently (n = 20) before and after the stimulation program

Development	Sat with support group (n = 20)					Sat independently group (n = 20)				
	Before	After	Difference	*p*-value	Effect size (d_{cohen})	Before	After	Difference	*p*-value	Effect size (d_{cohen})
CSBS-DP scores	84.8 ± 12.1	86.2 ± 15.6	1.45 ± 12.5	0.587	0.10	84.2 ± 13.8	86.6 ± 16.2	2.4 ± 12.3	0.354	0.16
- Social	10.2 ± 2.8	10.1 ± 2.9	-0.1 ± 2.7	0.714	0.01	9.85 ± 2.7	9.8 ± 3.1	0 ± 2.6	0.979	0.02
- Speech	6.8 ± 2.2	6.8 ± 2.7	0 ± 2.6	0.909	-[#]	6.75 ± 2.6	7.0 ± 2.9	0.2 ± 3.0	0.908	0.09
- Symbolic	4.3 ± 0.9	5.2 ± 2.2	0.9 ± 2.3	0.128	0.54	4.5 ± 1.1	5.5 ± 2.6	0.9 ± 2.1	0.072	0.50
AIMS scores	29.4 ± 4.6	39.2 ± 7.3	9.9 ± 5.5	0.001[**]	1.61	40.4 ± 7.5	47.4 ± 6.3	7.2 ± 3.4	0.001[**]	1.01
- Supine	8.4 ± 0.5	9.0 ± 0.2	0.6 ± 0.5	0.001[**]	1.58	9.0 ± 0.0	9.0 ± 0.0	0.0 ± 0.0	-[#]	-[#]
- Prone	12.8 ± 2.1	15.6 ± 2.2	2.8 ± 1.8	0.001[**]	1.30	16.2 ± 1.8	19.3 ± 2.3	3.1 ± 2.1	0.001[**]	1.50
- Sitting	5.9 ± 2.7	9.6 ± 2.7	3.7 ± 2.6	0.001[**]	1.37	10.5 ± 2.2	11.7 ± 0.7	1.2 ± 2.0	0.051	0.74
- Standing	2.7 ± 1.8	5.2 ± 2.9	2.5 ± 2.5	0.002[**]	1.04	5.9 ± 2.7	8.8 ± 2.8	2.9 ± 2.2	0.008[**]	1.05

Note: CSBS-DP, The Communication and Symbolic Behavior Scales-Developmental Profile Infant Toddler Checklist; AIMS, Alberta Infant Motor Scale. Total raw scores of the AIMS = 58 scores, supine 9 scores, prone 21 scores, sitting 12 scores, and standing 16 scores. Total standard scores of the CSBS-DP = 135 scores, and each composite = 17 scores. The Wilcoxon signed-rank test was used to analyze the CSBS-DP scores of both groups and the AIMS of the sat independently group, while the paired t-test was used to analyze the AIMS scores of the sat with support group. [*] Significant difference (*p*-value < 0.05); [**] Significant difference (*p*-value < 0.01) [#] data could not be analyzed due to the same value of mean.

Discussion

The objective of the current study was to compare the language and gross motor scores before and after stimulation programs in infants who sat with support and in infants who sat independently. Results from the table 2 of our study did not support the hypothesis that through gross motor developmental stimulation in upright structured play during sitting skill attainment, healthy orphaned infants would exhibit simultaneous improvement in language development scores during the attainment of sitting skills.

The non-significant improvement in language development suggested that through structured play stimulation, their language skills could be independently developed. It could need more than 4 weeks for language skills to be stimulated. Although research evidence has found significant relationships between language and gross motor development[7,11,14,15,16], Darrah et al[23] found that the acquisition of each developmental domain is independent in rate of development. Another reason for a non-significant difference of language scores could be an inadequate sample size of participants leading to a small power of test, approximately 8-10% of both groups.

According to a number of studies[24,25], infants aged from 6 months up to the end of their first year were able to attain new skills related to being upright, such as crawling, sitting, pulling to stand, cruising, and finally walking independently. At this age range, a child is able to independently control the lower body and pelvis in conjunction with the development of upper trunk or upper chest motor skills[18]. After a four-week period of the stimulation program, both groups of infants in the orphanage recruited in this study displayed typically developing gross motor skills, especially independent sitting, according to the range of age from the WHO study[8]. From table 2, infants who were recruited when they sat with support significantly improved in all sub-scale scores of gross motor development measured using the AIMS, while infants who sat independently continued to significantly achieve their gross motor scores in prone and standing positions. The non-significant increase in scores in the supine and sitting positions in this group could come from the ceiling effect of the AIMS measurement.

For children in orphanages who tend to have language developmental delay[3,5], we support the concept of stimulating development that there is no need to wait until infants are able to sit independently before their language skills are stimulated. It is implied that the stimulation of language skills can begin when infants are able to control their head, neck, and upper trunk in an upright posture or in a pelvic-support seated posture. A previous study[26] suggests that the onset of unsupported sitting initiates a period of exploration and change in infant vocalization. When infants are first able to maintain an upright sitting position, they "discover" new possibilities for vocal production in the very act of vocalizing[26].

Furthermore, the period of learning to sit independently may be critical to promote an optimal environment that is conducive to language development. Postural control development, especially in sitting, is important for motor milestones. Greco et al[27] mentioned that infants at the age of six to seven months display trunk control by modifying direction-specific adjustments to suit the situation at the thoracic level. It is suggested that once an infant has begun to babble, providing infants with trunk control in sitting would create the context for improving language skills[27]. In addition, improvement of trunk control in the sitting sub-scale could help attain visual capacity and acts as a composition of input and perception in part of language and cognition[26].

The hypothesis of this study was not verified, and the current study contains several limitations. Infants were recruited conveniently from an orphanage located in the northeastern part of the country. The sample size was small which contained low power of test of the findings. It is suggested that in order to investigate the

effect of a stimulation program of structured play in upright positions, a larger sample size with a design of a randomized control trial is needed. The stimulation program, especially for language development, could be performed for a longer period. The fact that the study examined the outcomes after the four-week intervention was another limitation for the measurement of language development, future studies should consider a longer follow-up of gross motor and communication development until infants attain their development at the end of their first year of life.

Conclusions

A stimulation program for language and gross motor development would be beneficial for healthy infants being raised in an orphanage, which could be started when infants still sat with support. This study found likely increased scores for language development after orphaned infants received the stimulation program during sitting attainment. The study suggests that the time before the onset of independent sitting or when infants are about to sit could be good for orphaned infants to promote their language and gross motor skills by providing more upright play and interaction with caregivers.

Take home messages

Healthy orphaned infants showed non-significant improvement in language development through the a four-week gross motor stimulation program during the period of acquiring independent sitting skills. Nevertheless, infants who live in deprived environments should undergo language skill stimulation before they acquire independent sitting skills. A combination of stimulation programs for gross motor and language development should be implemented for infants raised in orphanages.

Conflicts of interest

The authors declare no conflicts of interest.

Acknowledgments

The authors would like to thank all infants, staff, and the Directors of Children's homes for their contributions during data collection. This research was funded by the Graduate School Research Fund, Khon Kaen University, Thailand.

References

1. Prommin S, Bennett S, Mato L, Siritaratiwat W. Longitudinal assessments of gross motor development in orphaned infants. J Med Tech Phy Ther 2017; 29(3): 337-49.
2. Prommin S, Bennett S, Keeratisiroj O, Siritaratiwat W. Instability of gross motor development during the first year in orphaned infants: A longitudinal observational study. Early Child Dev Care 2020; 190(13): 2041-9.
3. Worku BN, Abessa TG, Franssen E, Vanvuchelen M, Kolsteren P, Granitzer M. Development, social-emotional behavior and resilience of orphaned children in a family-oriented setting. J Child Fam Stud 2018; 27(2): 465-74.
4. Chaibal S, Bennett S, Rattanathanthong K, Siritaratiwat W. Early developmental milestones and age of independent walking in orphans compared with typical home-raised infants. Early Hum Dev 2016; 101: 23-6.
5. Hearst MO, Himes JH, Johnson DE, Kroupina M, Syzdykova A, Kroupina M, et al. Growth, nutritional, and developmental status of young children living in orphanages in Kazakhstan. Infant Ment Health J 2014; 35(2): 94-101.
6. Rachwani J, Santamaria V, Sandra L, Saavedra SL, Wood S, Porter F, et al. Segmental trunk control acquisition and reaching in typically developing infants. Exp Brain Res 2013; 228(1): 131-9.
7. Libertus K, Violi DA. Sit to talk: Relation between motor skills and language development in infancy. Front Psychol 2016; 7: 475.

8. WHO Multicentre Growth Reference Study Group. WHO motor development study: Windows of achievement for six gross motor development milestones. Acta Paediatr 2006; 95: 86-95.
9. Van Balen LC, Dijkstra LJ, Hadders-Algra M. Development of postural adjustments during reaching in typically developing infants from 4 to 18 months. Exp Brain Res 2012; 220(2): 109-19.
10. Adolph KE, Karasik LB, Tamis-LeMonda CS. Moving between cultures: Cross-cultural research on motor development. In Bornstein M, editor. Handbook of cross-cultural developmental science, New York; 2010. p.1-23.
11. Oudgenoeg-Paz O, Volman MCJ, Leseman PP. Attainment of sitting and walking predicts development of productive vocabulary between ages 16 and 28 months. Infant Behav Dev 2012; 35(4): 733-6.
12. Alcock KJ, Krawczyk K. Individual differences in language development: Relationship with motor skill at 21 months. Dev Sci 2010; 13(5): 677-91.
13. Houwen S, Visser L, van der Putten A, Vlaskamp C. The interrelationships between motor, cognitive, and language development in children with and without intellectual and developmental disabilities. Res Dev Disabil 2016; 53: 19-31.
14. He M, Walle EA, Campos JJ. A cross-national investigation of the relationship between infant walking and language development. Infant 2015; 20: 283-305.
15. Schwartz ER. Speech and language disorders. In: Schwartz MW, editor. Pediatric Primary Care: A Problem-Oriented Approach. St. Louis: Mosby; 1990. p. 696-700.
16. Muluk NB, Bayoglu B, Anlar B. A study of language development and affecting factors in children aged 5 to 27 months. Ear Nose Throat J 2016; 95: 23-9.
17. Darrah J, Redfern L, Maguire TO, Beaulne AP, Watt J. Intra-individual stability of rate of gross motor development in full-term infants. Early Hum Dev 1998; 52(2): 169-79.
18. Piper MC, Pinnell LE, Darrah J, Maguire T, Byrne PJ. Construction and validation of the Alberta Infants Motor Scale (AIMS). Can J Public Health 1992; 83: S46-50.
19. Taneja V, Aggarwal R, Beri RS, Puliyel JM. Not by bread alone project: A 2-year follow-up report. Child Care Health Dev 2005; 31: 703-6.
20. Wetherby AW, Allen L, Cleary J, Kublin K, Goldstein H. Validity and reliability of the Communication and Symbolic Behavior Scales Developmental Profile with very young children. J Speech Lang Hear Res 2002; 45: 1202-18.
21. Aimsamrarn P, Janyachareon T, Rattanathan-thong K, Emasithi A, Siritaratiwat W. Cultural translation and adaptation of the Alberta Infant Motor Scale Thai version. Early Hum Dev 2019; 130: 65-70.
22. Fowler J, Jarvis P, Chevannes M. Practical statistics for nursing and health care. UK: John Wiley and Sons; 2021.
23. Darrah J, Senthilselvan A, Magill-Evans, J. Trajectories of serial motor scores of typically developing children: Implications for clinical decision making. Infant Behav Dev 2009; 32(1): 72-8.
24. Wijnhoven TM, de Onis M, Onyango AW, Wang T, Bjoerneboe GE, Bhandari N. WHO Multicentre Growth Reference Study Group. Assessment of gross motor development in the WHO Multicentre Growth Reference Study. Food Nutr Bull 2004; 25: 37-45.
25. Onis M. WHO motor development study: Windows of achievement for six gross motor development milestones. Acta Paediatr 2006; 95: 86-95.
26. Harbourne RT, Ryalls B, Stergiou N. Sitting and looking: A comparison of stability and visual exploration in infants with typical development and infants with motor delay. Phys Occup Ther Pediatr 2014; 34(2): 197-212.
27. Greco ALR, da Costa CSN, Tudella E. Identifying the level of trunk control of healthy term infants aged from 6 to 9 months. Infants Behav Dev 2018; 50: 207-21.

ORIGINAL ARTICLE

Arch AHS

Archives of Allied Health Sciences 2023; 35(3): 11-22.

Detection of anti-MICA*010 in plasma of kidney transplant patients with pathologically confirmed antibody-mediated rejection

Sonwit Phanabamrung[1,2], Cholatip Pongskul[3], Chanvit Leelayuwat[2,4*]

[1] Biomedical Science program, Graduate School, Khon Kaen University, Khon Kaen, Thailand.
[2] Department of Clinical Immunology and Transfusion Sciences, Faculty of Associated Medical Sciences, Khon Kaen University, Khon Kaen, Thailand.
[3] Division of Nephrology, Department of Medicine, Faculty of Medicine, Khon Kaen University, Khon Kaen, Thailand.
[4] The Centre for Research and Development of Medical Diagnostic Laboratories, Faculty of Associated Medical Sciences, Khon Kaen University, Khon Kaen, Thailand.

KEYWORDS
Recombinant protein;
Protein purification;
MICA*010;
Antibody-mediated rejection;
Kidney transplantation.

ABSTRACT

The screening for major histocompatibility complex class I- chain related A (MICA) antibodies in pre- and post-kidney transplantation is crucial to minimize the risk of immunological complications and antibody-mediated kidney rejection (AMR). However, the conventional method for detecting anti-MICA antibodies does not include all relevant MICA, especially MICA*010, a predominant MICA allele in northeastern Thais (NETs). Moreover, a significant number of patients have been diagnosed with AMR despite the absence of detectable antibodies. We hypothesized that anti-MICA*010 might be responsible for rejection in such instances. The household recombinant MICA*010 protein was successfully produced by HEK293 T cells and purified by using a cobalt-based magnetic bead with the percent recovery of 88.994. The ELISA testing using purified MICA*010 proteins was performed on plasma samples from 122 patients who were pathologically confirmed with AMR. Our findings showed that 21 samples (17.21%) in AMR patients exhibited the presence of anti-MICA*010. The flow cytometry showed a concordant result with ELISA. Among these samples with anti-MICA*010, the co-existing anti-HLA antibody was observed in one sample. Furthermore, there were six patients (4.9%) with positive for ELISA were negative for both anti-HLA and other anti-MICA antibodies as identified by Lab Screening Mix (LSM) Luminex test suggesting the importance of anti-MCIA*010 detection. Although further research with the comprehensive evaluation regarding the involvement of anti-MICA*010 in the kidney rejection episode is still needed, the present study is the first to highlight the presence of this antibody, which could offer valuable information for antibody detection in the future.

***Corresponding author:** Chanvit Leelayuwat, MT, PhD. Department of Clinical Immunology and Transfusion Sciences, Faculty of Associated Medical Sciences, Khon Kaen University, Khon Kaen, Thailand. Email address: chanvit@kku.ac.th
Received: 5 June 2023/ Revised: 26 July 2023/ Accepted: 4 August 2023

Introduction

Kidney transplantation provides superior benefits in both survival and quality of life compared to undergoing regular dialysis treatment. Despite the advantages of kidney transplantation, the primary hindrance to its success is the incompatibility between the donor's tissue and the recipient's immune responses, which could result in graft failure via cellular-mediated rejection (CMR) or antibody-mediated rejection (AMR). AMR is caused by the preformed and/or de novo antibodies of patients that are specifically bound to the incompatible antigenic determinant found on the kidney tissue. In addition to the human leukocyte antigen (HLA), the major histocompatibility complex class I- chain related A (MICA) is considered one of the most important non-HLA antigenic molecules that play a critical role in kidney transplant rejection[1,2]. MICA is generally non-expressed in normal tissue. However, the upregulation of the MICA protein is found in various conditions including viral and bacterial infections, heat shock and DNA damage responses, oncogenic transformations, autoimmune conditions as well as inflammation[3]. Moreover, MICA has been found to be expressed on the renal tubular epithelial cells in response to ischemia-reperfusion injury, which might be occurred during the transplantation process, through the HIF-1α pathway[4].

Due to the extensive polymorphism of MICA proteins, antibody screening is necessary and routinely performed in pre- and post-kidney transplantation to investigate the cause of kidney rejection. As the MICA genotype is varied between ethnic groups, the antibodies produced by the recipient may be different. Several technologies have been developed for anti-MICA detection, such as ELISA and Luminex®[5,6]. Although the Luminex is widely acknowledged as the preferred method for MICA antibody testing, its capability to detect antibody specificity is limited which depends on the recombinant MICA protein immobilized on the beads. As a result, certain MICA alleles, such as MICA*010, are not included by this approach. The MICA*010 has been noted as an unexpressed MICA allele for decades due to a single amino acid substitution (proline for arginine) at position 6 in the first ß-strand of the α1 domain[7]. On the contrary, the study in our group found that the MICA*010 is certainly expressed on the cell surface (in preparation). In addition, this MICA allele is predominantly found (18.2%) in the northeastern Thais (NETs) and was shown to be significantly different from those of the Japanese and Caucasian populations (10.8% and 5.0%, respectively)[8]. Moreover, there are a large proportion of patients who have pathologically confirmed AMR with no detectable antibodies against HLA and/or MICA[9-11]. This indicates the inadequacy of current methods to comprehensively identify the relevant antibody that might contribute to kidney rejection. This information sparks the idea regarding the relevance of anti-MICA*010 in the AMR mechanism, particularly in cases of AMR without detectable antibodies, and requires further elucidation.

In the present study, the recombinant MICA*010 protein was produced and purified for the purpose of anti-MICA*010 detection in the patient's plasma. The plasma samples collected from histopathological proven AMR patients were screened for the presence of anti-MICA*010 by ELISA. Although the association between anti-MICA*010 and kidney transplant outcome is still unclear, our finding is the first study to demonstrate the existence of anti-MICA*010 in the plasma of patients which provides valuable information for further studies.

Materials and methods

Plasma samples

The 122 left-over plasma samples of patients who were pathologically diagnosed with antibody-mediated rejection (AMR) from Srinagarind Hospital were tested for the presence of the anti-MICA*010 antibody (the project was approved by Khon Kaen University Ethics

Committee for Human Research, HE601437). AMR was determined based on the classification guidelines provided by Banff 2017. To diagnose AMR, it was necessary to meet at least two out of the following three criteria: (i) histologic evidence of acute tissue injury; (ii) evidence of current/recent antibody interaction with vascular endothelium; and (iii) serologic evidence of DSA to HLA or other antigens, C4d staining or expression of validated transcripts/classifiers.

Construction of MICA*010 containing plasmid

The plasmid DNA carrying a soluble form of MICA*010 protein (sMICA*010) was generated by introducing a stop codon into the MICA*010 in the front of the transmembrane domain. MICA*010 was amplified from human genomic DNA (3 healthy subjects who possess homozygous MICA*010 that were obtained from the Liver Fluke and Cholangiocarcinoma Research Center, Khon Kaen University with informed consent (HE571283) by the PCR method. The sequences of forward and reverse primers for MICA*010 amplification are shown in table 1. The amplification cycles were 94°C for 2 min, then 30 cycles of 95°C for 30 sec, 60°C for 45 sec and 65°C for 2 min followed by 65°C for 10 min using the thermal cycler with 2 mM of $MgSO_4$. The PCR products were run in an agarose gel electrophoresis and subsequently purified from gel using the GFX gel band purification kit in accordance with the manufacturer's guidelines. The purified sMICA*010 gene was then ligated to the expression vector (pcDNA™3.1/V5-His TOPO™ TA Expression Kit) according to the manufacturer's instructions. The MICA*010 carrying plasmid was then transformed into a bacterial cell line (TG1) to amplify the plasmid DNA and purification. The plasmid DNA that carries the sMICA*010 gene was purified and verified by PCR-SSP[12,13] and nucleotide sequencing.

Table 1 Nucleotide sequences and annealing temperature of forward and reverse primer for soluble MICA*010 construction

Primer name	Primer sequence (5'→ 3')	Annealing temperature
F_Stop_sMICA010	CACC*ATGGGGCTGGGCCCGGTCTTCCTGCTTCTGGCTGGCATCT TCCCTTTTGCACCTCCGGGAGCTGCTGCTG*<u>**AGCCCCACAGTCT TCCTT**</u> (92 bases, binding site = 18 bases)	60 °C
R_Stop_sMICA010	CTA<u>ATGGTGGTGGTGATGATG</u>**CTGAAGCACCAGCACTTT** (39 bases, binding site = 18 bases)	60 °C

Note: Bold letters = binding site, Italics = leader sequence, Underline character = 6X-Histidine, CACC = TOPO sequence (necessary to integrate the interested gene into TOPO vector)

Transfection of sMICA*010 plasmid to HEK 293T cells

The sMICA*010 carrying plasmid was transfected into HEK 293T cells, which were cultured overnight in Dulbecco's modified eagle medium (DMEM) supplemented with 10% fetal bovine serum (FBS) and 1% pen-strep antibiotics. X-treme GENE HP DNA transfection reagent was used to transfect the plasmid following the manufacturer's instructions. As a control, an empty plasmid (pcDNA 3.1) was also transfected (MOCK). A household plasmid encoding the green fluorescence protein (GFP) was transfected in parallel to assess the transfection efficiency. The

transfection efficiency was investigated after 48 h of transfection using flow cytometry. The transfected cells were collected 72 h post-transfection for purification of soluble MICA*010 protein.

Recombinant MICA*010 protein collection and purification

The transfected HEK 293T cells were detached from the cell culture plates by repetitive up-and-down pipetting until all cells were completely detached from the culture plate. The cells were lysed by using the lysis buffer and subsequently centrifuge at 8,000 rpm for 10 min to provide an appropriate supernatant for the purification. The Dynabeads™ His-Tag Isolation & Pulldown utilizes cobalt-based immobilized metal affinity chromatography (IMAC) chemistry on the magnetic beads to specifically bind histidine-tagged proteins. The purification steps including MICA*010 protein binding to the cobalt-immobilized magnetic bead followed by three times of washing, and two times of elution step. In each step, the supernatant was carefully collected by aspiration at 2 min after the tube was placed on the magnet. All fractions, including crude, flowthrough, wash 1 and 2, eluate 1 and 2, were collected and used to verify the efficiency of protein purification. The purification process is shown in figure 1. The protein purity was investigated by running the SDS-PAGE and western blot.

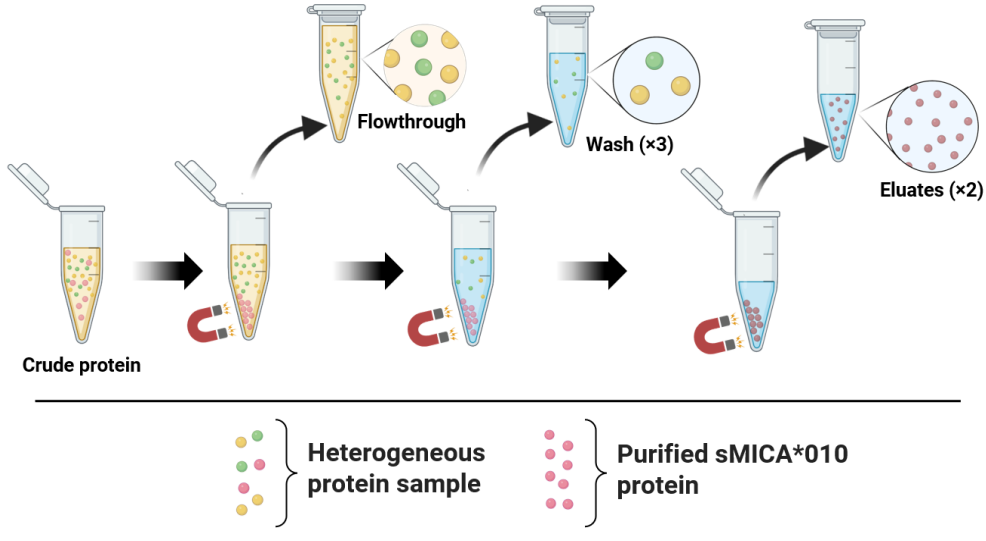

Figure 1 The illustration of protein purification processes using Dynabeads™ His-Tag Isolation & Pulldown. The purification steps including MICA*010 protein binding to the cobalt-immobilized magnetic bead, washing step and elution step.

Determination of the purity of purified MICA*010 protein by western blot

The purity of the purified protein was assessed by using western blot method. The concentration of all fractions was determined before running the western blot by using the BCA assay kit according to the manufacturer's instructions. The percent recovery of a protein production process was calculated by comparing the amount of the target protein recovered at the end of the process to the amount of protein that was initially present in the starting crude. The formula for calculating the percent recovery is as follows:

% Recovery = (Amount of pure MICA*010 protein recovered/Amount of starting crude protein) x 100%

All fractions, including crude MICA*010 protein, flowthrough, wash fraction and eluates, obtained from the purification process were run in the 12.5% polyacrylamide gel with 150 volts for 90 min. The gel was cut and blot to the polyvinylidene difluoride (PVDF) membrane to transfer all the protein to the membrane using semi-dry method (300 volts, 80 min). After that the membrane was washed 1 time with 0.1% Tween-20 in Tris-Buffered Saline (TBS-T). The membrane was blocked with 5% skim milk prepared in 0.1% TBS-T at RT for 1 h. The membranes were separately incubated with 0.5 µg/mL of anti-MICA (clone WJ-1, household) or anti-6X Histidine (Biolegend, SD, CA) for overnight at 4 °C with shaker. The membranes were washed 3 times with 0.1% TBS-T and probed with the secondary antibody (HRP-labelled goat anti-mouse IgG (Biolegend, SD, CA) in the dilution of 1:1,000 prepared in blocking buffer) at RT for 1 h. After this, the membranes were washed 3 times and detected by using ECL western blot detection kit (Cytiva, MA, USA).

Detection of anti-MICA*010 in patients' plasma using ELISA

The ELISA method was developed for anti-MICA*010 detection. In brief, the ELISA plate was coated with 3 µg/well of purified sMICA*010 protein prepared in carbonate-bicarbonate buffer, pH 9.8 for overnight at 4°C. After washing with 0.2% PBS-T to remove unbound proteins, 300 µL of blocking buffer (5% skim milk prepared in 0.1% PBS-T) was added to each well and subsequently incubated at 37°C for 2 h in order to block free area of the ELISA plate. 100 µL of diluted plasma samples (dilution of 1:100 with 3% skim milk) were added and incubated at 37ºC for 1 h. Subsequently, washed and added the HRP-tagged goat anti-human IgG (Biolegend, SD, USA) at the dilution 1:5,000 in 2% skim milk for 1 h at 37ºC. Then, the conjugated antibody was removed by flicking the plate over a sink and after 3 washing with washing buffer, 100 µL of 3,3',5,5'-Tetramethylbenzidine (TMB) substrate solution was added for 1 h in the dark at room temperature. The absorbance was measured at 450 nm by microplate reader (Sunrise™, Tecan, Männedorf, Switzerland). The cut-off value was defined as mean + 2SD of the absorbance (OD450) obtained from the plasma of 50 healthy donors. The positive or negative was defined by using the established cut-off value.

Establishment of flow cytometry to verify the presence of anti-MICA*010 in patients' plasma

The experiment was conducted using HEK 293T cells transfected with the MICA*010 plasmid (intact form) and simultaneously transfected with an empty plasmid (pcDNA 3.1) as a mock control. The cells were harvested 48 h after transfection, washed with sterile 1X PBS, and blocked with 500 µL of blocking buffer (consisting of 20% AB normal serum and 2% FBS in sterile 1X PBS) for 15 minutes. After washing, each dilution of the patient's plasma ranging from 0 (PBS buffer) to 1:100 was separately incubated with the MICA*010 or MOCK transfectants on ice for 1 hour. For the pioneering study, three plasma samples from healthy donors and two from kidney transplant patients that showed positive result from ELISA (no. DSA20 and DSA23) were used. The cells were then washed, and 5 µL of goat anti-human IgG labeled with Allophycocyanin (APC) was added for a 30-minute incubation on ice. After final washing with 1X PBS, the cells were analyzed using flow cytometry. The mean fluorescence intensity (MFI), which is a measure of the amount of fluorescence emitted by a sample, was measured for each transfectant after incubation with the plasma samples. The MFI values obtained for the MICA*010 and MOCK transfectants were compared to determine the presence of anti-MICA*010 in the patient's plasma.

Results

Cloning of the MICA*010 gene to the expression vector for protein production

To obtain the soluble form of the MICA*010 protein, MICA*010 was amplified from human genomic DNA (3 subjects from our previous study who were identified as a MICA*010/010 genotype

by a PCR-SSP). As shown in figure 2A, the expected PCR product size appeared at 1898 bp which was found in all three samples. PCR products were cut and purified. Then, cloning into the expression vector (pcDNA 3.1) and subsequently verified by PCR-SSP (Figure 2B). The interpretation of the PCR-SSP for MICA genotyping dictates that the MICA*010 allele should have positive bands in reactions 3, 5, 8, and 9[12,13]. Additionally, homozygous MICA*010 individuals must exhibit negative bands when tested with primer mixture 4, which is specific for the MICA*019 allele. This result indicates the appearance of the MICA*010 gene inserted in the purified plasmid DNA extracted from the bacterial clone. The result was finally confirmed by DNA sequencing. The amino acid sequence of three extracellular domains (exon 2, 3 and 4) of MICA*010 inserted in the plasmid DNA was identical to that of the sequence retrieved from the HLA/MICA database (http://hla.alleles.org/data/mica.html; Release version 3.44.0, 13 January 2022) as shown in figure 2C. All of these findings support the successful cloning of the MICA*010 (exons 2-4) into the expression vector pcDNA 3.1 for the production and purification of protein.

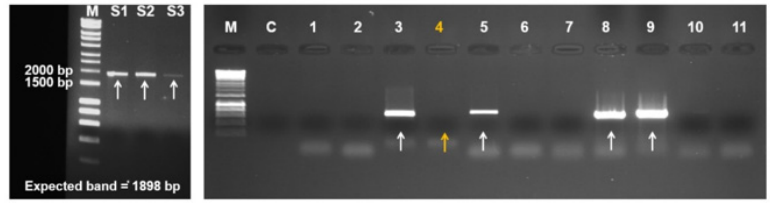

(A)

(B)

```
                    ....|....| ....|....| ....|....| ....|....| ....|....|
                         5         15         25         35         45
MICA*010 (from database) EPHSLPYNLT VLSWDGSVQS GFLAEVHLDG QPFLRYDRQK CRAKPQGQWA
sMICA*010 (Sequencing)   EPHSLPYNLT VLSWDGSVQS GFLAEVHLDG QPFLRYDRQK CRAKPQGQWA

                    ....|....| ....|....| ....|....| ....|....| ....|....|
                        55         65         75         85         95
MICA*010 (from database) EDVLGNKTWD RETRDLTGNG KDLRMTLAHI KDQKEGLHSL QEIRVCEIHE
sMICA*010 (Sequencing)   EDVLGNKTWD RETRDLTGNG KDLRMTLAHI KDQKEGLHSL QEIRVCEIHE

                    ....|....| ....|....| ....|....| ....|....| ....|....|
                       105        115        125        135        145
MICA*010 (from database) DNSTRSSQHF YYDGELFLSQ NLETEEWTVP QSSRAQTLAM NVRNFLKEDA
sMICA*010 (Sequencing)   DNSTRSSQHF YYDGELFLSQ NLETEEWTVP QSSRAQTLAM NVRNFLKEDA

                    ....|....| ....|....| ....|....| ....|....| ....|....|
                       155        165        175        185        195
MICA*010 (from database) MKTKTHYHAM HADCLQELRR YLESSVVLRR TVPPMVNVTR SEASEGNITV
sMICA*010 (Sequencing)   MKTKTHYHAM HADCLQELRR YLESSVVLRR TVPPMVNVTR SEASEGNITV

                    ....|....| ....|....| ....|....| ....|....| ....|....|
                       205        215        225        235        245
MICA*010 (from database) TCRASSFYPR NIILTWRQDG VSLSHDTQQW GDVLPDGNGT YQTWVATRIC
sMICA*010 (Sequencing)   TCRASSFYPR NIILTWRQDG VSLSHDTQQW GDVLPDGNGT YQTWVATRIC

                    ....|....| ....|....| ....|....| ....|...
                       255        265        275        285
MICA*010 (from database) RGEEQRFTCY MEHSGNHSTH PVPSX----- -------X
sMICA*010 (Sequencing)   RGEEQRFTCY MEHSGNHSTH PVPSESAGAS ASSPPPLX
```

(C)

Figure 2 The analysis of sMICA*010 clone (A) The PCR bands investigated by an agarose gel electrophoresis. The amplified MICA gene from each individual; M, DNA marker; S1, subject 1; S2, subject 2; S3, subject 3. (B) The PCR-SSP result of the MICA*010 inserted plasmid using 11 primer mixtures, M, DNA marker; C, negative control; number 1 – 11 represent the number of primer mixtures used for the PCR-SSP. (C) The alignment of the amino acid sequence of the MICA*010 protein. The amino acid sequence of the MICA*010 retrieved from the HLA/MICA database aligned with the plasmid DNA sequencing. Exons 2, 3 and 4 were highlighted in the yellow, red and green boxes, respectively.

Production and purification of recombinant MICA*010 protein and verification of protein purity

The plasmid DNA encoding green fluorescence protein (GFP) was simultaneously transfected to examine the transfection efficiency. The GFP transfectant revealed the high efficiency of plasmid transfection to the HEK 293T cells with 70-90% of the transfection efficiency as measured by flow cytometry (Figure 3A). After 72 h of transfection, the sMICA*010 transfected cells were collected. All fractions including crude, flowthrough, wash and eluates were collected and stored at -20 °C for further use. The protein concentration was determined by the BCA protein assay (Thermo Scientific, MA, USA). Evidently, the purification process provides a high percent recovery at 88.994%. In addition, the protein purity was assessed using SDS-PAGE and western blot. After probing with the anti-6X histidine or anti-MICA (clone WJ-1), the MICA-specific band appeared at around 50 kDa in both antibody clones. The Coomassie blue staining revealed more purity of the protein band when compared to the crude mock and crude MICA*010 protein (Figure 3B). It should be noted that, based on the principle of the protein purification kit that the His-tagged protein binds to the cobalt ions on the magnetic beads, other proteins with exposed histidine residues that are not part of a His-tag may also bind non-specifically to the beads. The non-specific protein was found after staining with both antibodies (Figures 3C and 3D). However, most of the protein in the eluates is occupied by the recombinant MICA*010 protein as demonstrated by the density of the band after staining with the specific anti-MICA antibody. Alternatively, these multiple bands stained by both antibodies could represent different forms of glycosylations. This indicated the applicability of the purified recombinant protein for further step.

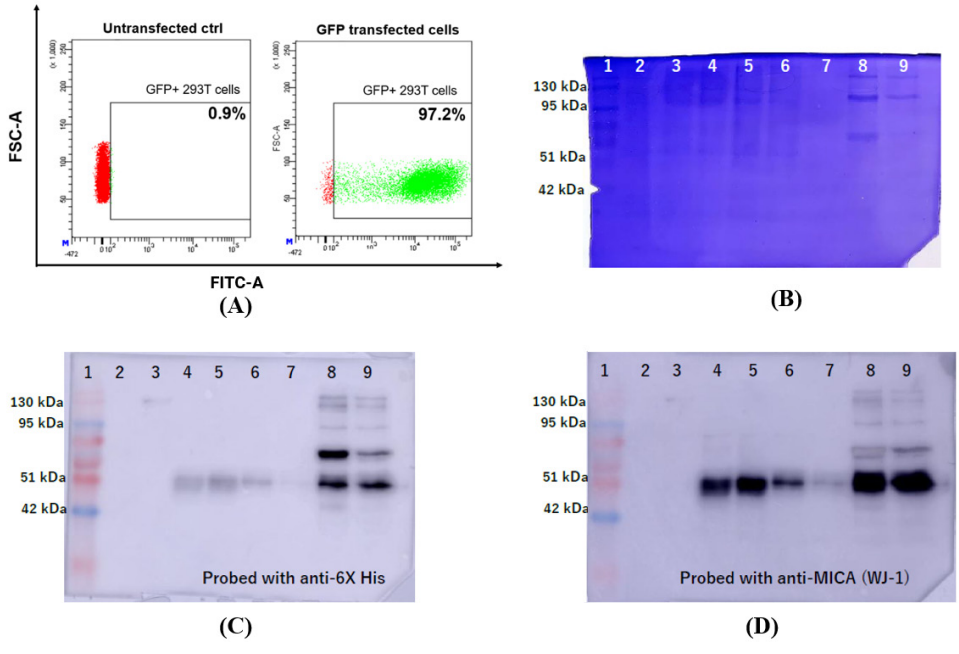

Figure 3 Evaluation of MICA*010 transfection and protein purity after protein purification process. (A) The transfection efficiency assessed by GFP transfection. (B) The polyacrylamide gel stained with Coomassie blue R-250 solution. (C) The western blot analysis which probed with anti-6X His. (D) The western blot analysis which probed with anti-MICA, clone WJ-1. All fractions of proteins were investigated under denaturing conditions in the presence of dithiothreitol (DTT) Lane 1, protein marker; lane 2, crude Mock; lane 3, crude ß-galactosidase; lane 4, crude MICA*010; lane 5, flowthrough; lane 6, wash 1; lane 7, wash 2; lane 8, eluate 1 and lane 9, eluate 2.

Detection of anti-MICA*010 in patients' plasma using developed ELISA method

To detect anti-MICA*010 in patients' plasma, the ELISA method was developed and tested on 50 healthy donor plasma samples to determine the cut-off value. The mean and standard deviation of the absorbance (OD450) from healthy donor plasma samples were calculated as 0.264 and 0.124, respectively. The cut-off value, which is defined by mean + 2SD of the healthy subjects, was determined to be 0.511. Plasma samples from 122 kidney transplant patients with AMR were then tested using this method. Among all samples, 21 samples (17.21%) showed an OD greater than the cut-off value (Figure 4A), indicating the presence of anti-MICA*010. The available data about the *MICA* genotype of both the donor and patient, as well as the anti-HLA profile of these 21 samples, were considered. The data regarding the anti-HLA and -MICA profiles of these samples was kindly obtained from the blood bank, Srinagarind Hospital. The complete LSM data were available for nine samples, which included both anti-HLA and anti-MICA antibodies. Additionally, there were ten samples that only had anti-HLA data, while LSM data were unavailable for two samples for either anti-HLA or anti-MICA antibodies. The data of Lab Screening Mix (LSM) Luminex test revealed two plasma samples, among 21 positive ELISA, showed positive signals. One sample had a positive result for bead no. 68, which detected MICA*001, *004, *012, *018 and 027, while the other sample had a positive result for bead no. 97, which detected MICA*002, *007, *009, *017 and *019. Although the incomplete dataset of the LSM Luminex test possess a limitation to our study, the identification of co-existing anti-MICA and anti-HLA class I and II antibodies in a particular sample (DSA23) suggests their involvement in the episode of kidney rejection through an antibody-mediated mechanism (Figure 4B).

Verification of anti-MICA*010 in patients' plasma using flow cytometry

To verify the ELISA result, flow cytometry was additionally performed. The limitation of this study is that the HEK 293T cells used in the experiment have internal MICA expression, which makes it difficult to accurately identify the true signal of anti-MICA*010 positive. To address this issue, the gap MFI signal (ΔMFI) between the MICA*010 transfectant and MOCK control (ΔMFI = $MFI_{MICA*010} - MFI_{MOCK}$) was a more accurate measure. As a result, by considering the ΔMFI (Figure 4C), it was clear that the ΔMFI found in the patient samples was higher than that of the healthy donors. The flow cytometry results showed the concordant pattern with the ELISA, verifying the appearance of an anti-MICA*010 in the plasma sample. However, this is a pioneering study, and further research with a greater number of samples is required. Moreover, to avoid the interference of the internal MICA expression, the mammalian cell line without MICA expression is recommended.

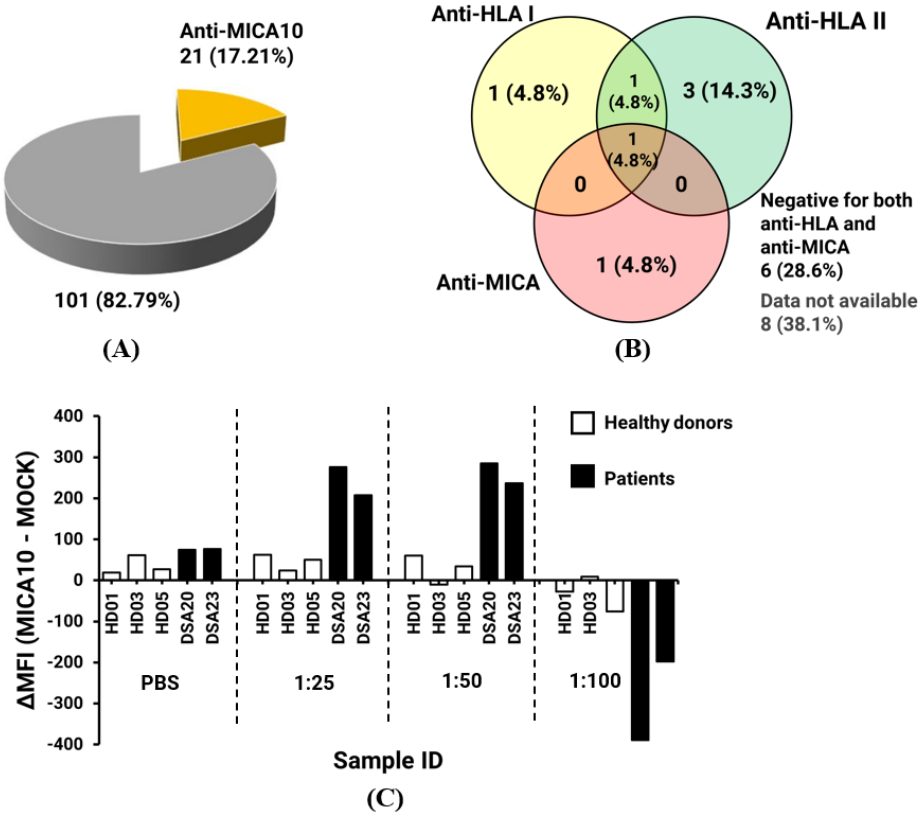

Figure 4 The detection of anti-MICA*010 in patient's plasma. (A) The percentage of the anti-MICA*010 detected by the developed ELISA method. (B) The distribution of anti-MICA and -HLA antibodies among the 21 plasma samples that were positive for ELISA. According to the available LSM data set, among 21 samples analyzed, one sample exhibited solely anti-HLA class I, three samples displayed anti-HLA class II, one sample demonstrated the presence of both anti-HLA class I and class II, one sample exhibited solely anti-MICA, one sample revealed the co-existence of anti-MICA along with anti-HLA class I and class II antibodies, six samples did not exhibit either anti-MICA or anti-HLA antibodies and data was not available in eight samples. (C) The ΔMFI of the anti-MICA*010 detection using flow cytometry presented in different plasma dilution including PBS (diluent), 1:25, 1:50 and 1:100. HD; healthy donor, DSA; patient plasma.

Discussion

Recently, the importance of the MICA protein in kidney transplantation has been acknowledged and extensively studied for its role in organ rejection. Studies suggest that anti-MICA antibodies binding to MICA molecules on endothelial cells in transplanted kidneys may affect transplantation outcomes[14,15]. The identification of anti-MICA antibodies prior to and after kidney transplantation relies on the Luminex technology, which can detect numerous MICA-specific antibodies, except the antibody against MICA*010. The antibody specific to this MICA allele is hypothesized to be involved in kidney rejection as it showed a high frequency in NETs population. To obtain purified protein for downstream applications, a six-histidine tag was added to the C-terminal of the soluble MICA*010 protein. The purification was performed by using Dynabeads™His-Tag Isolation and Pulldown, which

is the optimized cobalt-based immobilized metal affinity chromatography (IMAC). The magnetic beads were coated with the cobalt ion that has a higher binding affinity for the His-tag than nickel. This higher affinity can be attributed to the stronger interaction between cobalt and the imidazole ring of histidine residues, which provide higher purity and yield compared to nickel-based resins[16,17]. The purification kit enables the pursuit of MICA*010 protein in HEK 293T cells by reducing the background contamination of other irrelevant cellular proteins. Despite utilizing the His-tag purification method, there were still other protein bands visible on the stained polyacrylamide gel. This may be attributed to other cellular proteins with exposed histidine residues that are not part of the his-tag, which tend to bind non-specifically to the magnetic beads. Alternatively, these multiple bands stained by both antibodies against MICA*010 and histidine could represent different forms of glycosylations. Nonetheless, western blot analysis indicated that the MICA*010 protein occupied the majority of the protein in the eluates when the specific antibody against the MICA protein was employed. Additionally, the purification method employed in this study successfully retrieved the desired his-tagged MICA*010 protein, as evidenced by the desirable percent recovery, exceeding 80% in this research. Furthermore, to eliminate the influence of additional impure proteins that might lead to non-specific binding and erroneous positive results in the anti-MICA*010 detection, the crude protein acquired from the MOCK control was utilized in each experiment.

Our study found that the MICA*010 allele is certainly expressed on the cell surface (in preparation), suggesting its potential contribution to kidney transplant outcomes. This study aimed to investigate this contribution and found that patients with AMR exhibited the presence of anti-MICA*010 through the ELISA method. Results from flow cytometry showed a similar trend to the ELISA findings, where the ΔMFI in patient plasma was higher than that of healthy donors. Out of the 21 samples that were tested positive for anti-MICA*010 via ELISA, one sample displayed the co-existence with anti-HLA class I and class II. Previous studies have shown that the presence of both anti-HLA and anti-MICA antibodies in kidney transplant patients is associated with a longer time to reach optimal serum creatinine level after transplantation[18]. Meanwhile, six patients with the positive OD from ELISA were tested negative for both anti-HLA and other anti-MICA antibodies. This information suggests that monitoring for anti-MICA*010 should be beneficial, particularly in the instances where the patient has been diagnosed with AMR. This data indicate that the simultaneous detection of antibodies targeting both HLA and non-HLA antigens (especially of MICA) may provide a more thorough evaluation of the patient's immune responses to the kidney allograft and may assist in the categorization of immunological risk. The limitation of this study with respect to the identification of anti-MICA*010 through flow cytometry was the internal HLA-I and MICA expressions found in the HEK 293T cells. However, this could be addressed by employing the MOCK control, which would be sufficient to exclude such expression. To obtain more reliable results regarding the presence of anti-MICA*010, it is recommended to perform transfection in HLA and MICA deficient mammalian cell lines. There is a study that proposed the method to eliminate the expression of *HLA* and *MICA* gene in the HEK 293T cells through CRISPR/Cas9 system[19]. Moreover, the HLA class I and MICA/B null HEK 293T panel expressing single MICA alleles has been reported to provide beneficial in anti-MICA antibodies detection[20]. This pioneering study suggested the presence of anti-MICA*010 in the plasma of AMR patients which could be served as an initial point to emphasize the importance of this antibody in the future. However, for more understanding of the clinical relevance of anti-MICA*010 in kidney rejection, increasing patient numbers and a comprehensive investigation that includes other relevant factors are also necessary to consider thoroughly.

Conclusion

The anti-MICA plays an essential role in kidney rejection. Therefore, comprehensive antibody detection is crucial for minimizing the immunological risk and help assessing the cause of AMR. The MICA*010 allele has been found predominantly in NETs and was hypothesized to be involved in the AMR episode. In this study, we successfully produced the recombinant MICA*010 protein and used to establish the ELISA method for anti-MICA*010 detection. Our findings also illustrate the presence of anti-MICA*010 in the plasma of AMR patients. Moreover, the co-existence of anti-MICA*010 and anti-HLA antibodies was observed. The involvement of this antibody in the occurrence of AMR is still unclear. However, this research could be a groundbreaking to emphasize the significance of this antibody in future studies.

Take home messages

The existence of anti-MICA*010 in plasma samples of patients with AMR was demonstrated, which paves the foundation regarding the possible role of this antibody on the AMR episode and necessitates further comprehensive investigation.

Conflicts of interest

The authors declare no conflict of interest.

Acknowledgements

We gratefully acknowledge the Liver Fluke and Cholangiocarcinoma Research Center, Khon Kaen University for providing DNA samples of homozygous MICA*010 individuals. The authors also would like to thank Asst. Prof. Piyapong Simtong for coordinating in the collection of plasma samples and providing the information of anti-HLA and -MICA profiles detected by Lab Screening Mix (LSM). The MICA*010 inserted plasmid (intact form) was kindly obtained from Asst. Prof. Dr. Amonrat Jumnainsong. This work was financially supported by the Thailand Research Fund (TRF), the Royal Golden Jubilee (RGJ-PhD program) Scholarship (PHD/0009/2559) and National Research Council of Thailand through Khon Kaen University (2018-2019).

References

1. Zou Y, Stastny P, Süsal C, Döhler B, Opelz G. Antibodies against MICA antigens and kidney-transplant rejection. N Engl J Med 2007; 357(13): 1293–300.
2. Zwirner NW, Marcos CY, Mirbaha F, Zou Y, Stastny P. Identification of MICA as a new polymorphic alloantigen recognized by antibodies in sera of organ transplant recipients. Hum Immunol 2000; 61(9): 917–24.
3. Chen D, Gyllensten U. Review MICA polymorphism : biology and importance in cancer 2014; 35(12): 2633–42.
4. Luo L, Lu J, Wei L, Long D, Guo JY, Shan J, et al. The role of HIF-1 in up-regulating MICA expression on human renal proximal tubular epithelial cells during hypoxia/reoxygenation. BMC Cell Biol 2010; 11: 91.
5. Karam G, Kälble T, Alcaraz A, Aki FT, Budde K, Humke U, et al. Guidelines on renal transplantation. Ren Transplant - Eur Assoc Urol 2009; March: 327-37.
6. Picascia A, Infante T, Napoli C. Luminex and antibody detection in kidney transplantation. Clin Exp Nephrol 2012; 16(3): 373–81.
7. Li Z, Groh V, Strong RK, Spies T. A single amino acid substitution causes loss of expression of a MICA allele. Immunogenetics 2000; 51(3): 246–8.
8. Romphruk AV, Naruse TK, Romphruk A, Kawata H, Puapairoj C, Kulski JK, et al. Diversity of MICA (PERB11.1) and HLA haplotypes in Northeastern Thais. Tissue Antigens 2001; 58(2): 83–9.
9. Suneja M, Kuppachi S. Acute antibody-mediated renal allograft rejection associated with HLA-Cw17 antibody. CKJ Clin Kidney J 2012; 5: 254-6.

10. Sellares J, Reeve J, Loupy A, Mengel M, Sis B, Skene A, et al. Molecular diagnosis of antibody-mediated rejection in human kidney transplants. Am J Transplant 2013; 13: 971–83.
11. Irure J, López-Hoyos M, Rodrigo E, Gómez-Román J, Ruiz JC, Arias M, et al. Antibody-Mediated Rejection in Kidney Transplantation Without Evidence of Anti-HLA Antibodies? Transplant Proc 2016; 48: 2888-90.
12. Jumnainsong A, Romphruk AV, Jearanaikoon P, Klumkrathok K, Romphruk A, Luanrattanakorn S, et al. Association of polymorphic extracellular domains of MICA with cervical cancer in northeastern Thai population. Tissue Antigens 2007; 69(4): 326–33.
13. Romphruk AV, Romphruk A, Choonhakarn C, Puapairoj C, Inoko H, Leelayuwat C. Major histocompatibility complex class I chain-related gene A in Thai psoriasis patients: MICA association as a part of human leukocyte antigen-B-Cw haplotypes. Tissue Antigens 2004; 63(6): 547–54.
14. Risti M, Bicalho M da G. MICA and NKG2D: Is there an impact on kidney transplant outcome?. Front Immunol 2017; 8: 1–21.
15. Álvarez-Márquez A, Aguilera I, Gentil MA, Caro JL, Bernal G, Alonso JF, et al. Donor-specific antibodies against HLA, MICA, and GSTT1 in patients with allograft rejection and C4d deposition in renal biopsies. Transplantation 2009; 87(1): 94–9.
16. Porath J, Carlsson J, Olsson I, Belfrage G. Metal chelate affinity chromatography, a new approach to protein fractionation. Nature 1975; 258(5536): 598–9.
17. Porath J. Immobilized metal ion affinity chromatography. Protein Expr Purif 1992; 3(4): 263–81.
18. Sánchez-Zapardiel E, Castro-Panete MJ, Mancebo E, Morales P, Laguna-Goya R, Morales JM, et al. Early renal graft function deterioration in recipients with preformed anti-MICA antibodies: Partial contribution of complement-dependent cytotoxicity. Nephrol Dial Transplant 2016; 31(1): 150–60.
19. Hong CH, Sohn HJ, Lee HJ, Cho HI, Kim TG. Antigen presentation by individually transferred HLA class i genes in HLA-A, HLA-B, HLA-C null human cell line generated using the multiplex CRISPR-Cas9 system. J Immunother 2017; 40(6): 201–10.
20. Jeon JH, Baek IC, Hong CH, Park KH, Lee H, Oh EJ, et al. Establishment of HLA class I and MICA/B null HEK-293T panel expressing single MICA alleles to detect anti-MICA antibodies. Sci Rep 2021; 11(1): 1–12.

ORIGINAL ARTICLE

Arch AHS

Archives of Allied Health Sciences 2023; 35(3): 23-38.

Improved purification protocol for recombinant human leukocyte antigens using an affinity magnetic agarose

Thu Zar Ma Ma Moe Min[1,2,3], Sonwit Phanabamrung[3,4], Chanvit Leelayuwat[3,5*]

[1] Department of Medical Laboratory Technology, University of Medical Technology, Mandalay, Myanmar.
[2] Medical Technology Program, Faculty of Associated Medical Sciences, Khon Kaen University, Khon Kaen, Thailand.
[3] The Centre for Research and Development of Medical Diagnostic Laboratories (CMDL), Faculty of Associated Medical Sciences, Khon Kaen University, Khon Kaen, Thailand.
[4] Biomedical Sciences Program, Graduate School, Khon Kaen University, Khon Kaen, Thailand.
[5] Department of Clinical Immunology and Transfusion Sciences, Faculty of Associated Medical Sciences, Khon Kaen University, Khon Kaen, Thailand.

KEYWORDS
Recombinant HLA protein;
HEK 293T cell;
Protein expression;
Protein purification;
Anti-DYKDDDDK magnetic agarose method.

ABSTRACT

Anti-human leukocyte antigen (HLA) antibodies are a risk factor for graft failure and graft loss in organ transplantation. To develop a new biomolecular technique for anti-HLA antibody detection against HLA antigens, a large quantity of HLA proteins is necessary. The optimization of existing protein purification protocols plays a crucial role in laboratory practice in biomolecular technology. In this work, we presented the efficient expression of recombinant HLA-A and -B proteins in the HEK 293T cell line and an improved protocol of the PierceTM anti-DYKDDDDK magnetic agarose method for HLA protein purification to enhance the quantity of proteins. The percent recoveries of HLA-A and -B proteins were 81.15% and 80.73% at 350–380 µg/mL in the total eluates, respectively. The number of elution times and incubation time in the elution step were the most important to enhance the percent recovery and quantity of purified proteins. In conclusion, the improved purification protocol enables the high-yield production of functional recombinant HLA-A and -B proteins for the establishment of an ion-sensitive field-effect transistor-based immunosensor for anti-HLA antibody detection. Moreover, it could provide a useful guideline for the expression and purification of other DYKDDDDK-tagged recombinant proteins.

***Corresponding author:** Chanvit Leelayuwat, MT, PhD. Department of Clinical Immunology and Transfusion Sciences, Faculty of Associated Medical Sciences, Khon Kaen University, Khon Kaen, Thailand. Email address: chanvit@kku.ac.th
Received: 17 July 2023/ Revised: 4 August 2023/ Accepted: 30 August 2023

Introduction

The human leukocyte antigen (HLA) system is a cluster of related proteins that are encoded by the major histocompatibility complex (MHC) in humans. The MHC genes are divided into three subgroups: MHC class I, MHC class II, and central MHC or class III according to their locations on the human chromosome[1]. Among them, class I and class II genes are highly polymorphic and directly participated in antigen presentation. The HLA class I molecules: HLA-A, -B, and -C are expressed on the surface of a wide variety of nucleated cells with varying degrees of specificity. They are composed of three extremely polymorphic extracellular domains (α 1-3) and a transmembrane heavy chain associated with a light chain, β2-microglobulin (ß2-m). These cell-surface proteins are immunological barriers to organ and stem cell transplantations[2]. Antibody-mediated rejection (AMR) is strongly associated with graft failure and graft loss in renal transplantation and is caused by pre- and post-transplant HLA antibodies[3-5]. Therefore, detection and analysis of HLA-specific antibodies have become pivotal tasks in every clinical setting.

To set up a new biomolecular technique for anti-HLA antibody detection, a large quantity of HLA proteins is required. Moreover, the cost of commercial HLA proteins remains extremely high with their limited quantity, which is a major issue. Nowadays, many innovative technologies and high-quality protein purification kits manufactured by various suppliers have been introduced[6-8]. Among them, magnetic particle-based methods are frequently used in a wide range of biological applications due to their strong paramagnetic talent, low cost, simplified procedures, and short operating time. Moreover, multiple centrifugation steps are not required in the purification of the affinity-tagged protein utilizing magnetic nanoparticles[9-11].

Herein, the transfection efficiency of the lipofection method was systematically optimized by inserting the green fluorescent protein (GFP) plasmid into the HEK 293T cell line and determined by flow cytometry. In addition, we demonstrated an improved purification protocol that produced high yields of purified recombinant HLA-A*01:01 and -B*07:02 proteins using the commercial Pierce™ anti-DYKDDDDK magnetic agarose kit.

Materials and methods

Optimization of transfection efficiency of HLA-A and HLA-B plasmids

The optimization of transfection conditions was conducted using the plasmid encoding green fluorescence protein (GFP plasmid) according to the optimization protocol provided by the manufacturer of X-treme Gene HP DNA transfection reagent[12]. A constant plasmid DNA concentration was incubated with various amounts of transfection reagent. In this approach, a monolayer of 50,000 cells per well of HEK 293T cells with 70–90% confluency in a 24-well plate is transfected with 1 µg of DNA per well in varying amounts of transfection reagent (1 µL, 2 µL, 3 µL and 4 µL) at the 1:1, 2:1, 3:1, and 4:1 ratios of microliter (µL) transfection reagent to microgram (µg) of plasmid DNA.

The transfection efficiency of the GFP plasmid was evaluated by a flow cytometric method in which, a standard GFP-encoding plasmid was parallelly transfected alongside the HLA-A and -B plasmids. The ratio between the plasmid amount and the transfection reagent was varied to obtain the optimal ratio. After the transfection, the cells were incubated for 48 hours at 37°C in a 5% CO2 incubator allowing the green fluorescent protein expression. Following this incubation period, transfected cells were gently detached from the culture plate by repeated pipetting. A wash step was carried out, followed by centrifugation at 2,000 rpm for 5 mins. The cells were resuspended in the PBS buffer to obtain a single cell suspension.

The HEK 293T cells that had successfully taken up the GFP plasmid DNA and encoded it intracellularly demonstrated vivid green

fluorescence upon exposure to an excitation wavelength of approximately 488 nanometers (nm) measured by flow cytometer. To establish the threshold for distinguishing between GFP-positive and GFP-negative cells, we utilized untransfected HEK 293T cells as a reference.

Expression of HLA-A and HLA-B plasmids

HLA-A and -B plasmid DNA clones carry the cDNA sequences of HLA-A*01:01 (GenBank accession no. NM001242758) and HLA-B*07:01 (GenBank accession no. NM005514) in the pcDNA3.1+/C-(K)-DYK vector (GenEZ™ ORF clones) (Supplementary Figures S1A and S1B), which were expressed in HEK 293T cells as a tagged protein with a C-terminal DYKDDDDK tag. The transfection reagent, X-treme Gene HP DNA transfection reagent, and the optimized transfection protocol were used to transfect HLA-A and HLA-B-inserted plasmids into HEK 293T cells. The pcDNA3.1+/C-(K)-DYK without target HLA-A and -B cDNA was transfected into the cells as the MOCK control. The final volume of 100 µL of transfection mixture, containing 2 µL of the transfection reagent and 1 µg of each plasmid DNA and Dulbecco's Modified Eagle Medium (DMEM) media, was incubated for 15 min at room temperature and then added to HEK 293T cells (3.5×10^5 cells per well in a 6-well plate). For the large-scale production, five petri dishes were used for each experiment, and the final volume of 1000 µL of transfection mixture containing 18 µL of the transfection reagent, 12 µg of each plasmid DNA, and DMEM media was incubated for 15 min at room temperature. After that, transfection mixtures were plated onto HEK 293T cells (2.5×10^6 cells per petri dish), and cell culture plates were incubated at 37°C with 5% CO_2 for 72 h.

Optimization of DYKDDDDK-tagged HLA-A and -B proteins purification

The transfected HEK 293T cells were collected and lysed by ice-cold Pierce IP lysis buffer with protease enzyme buffer. Then, the lysate was centrifuged at 13,000 g for 10 min at 4°C. The supernatant was transferred to a new tube as crude proteins and Pierce™ Anti-DYKDDDDK Magnetic Agarose Kit was used to purify the DYKDDDDK-tagged HLA-A and -B proteins in the crude lysate. All purification steps, including binding the DYKDDDDK-tagged HLA proteins onto the magnetic beads, 3 times washing the beads with DYKDDDDK-tagged target proteins, and 3 times of elution steps for eluting the target protein from the beads were done to begin with the manufacturer's protocol (SOP1)[13]. Then, SOP1 was systemically optimized in each step of purification process because the C-terminal DYKDDDDK-tagged HLA-A and -B proteins were not successfully purified using SOP1.

Firstly, in SOP2 and 3, 100 µL of magnetic agarose slurry and 500 µL of binding buffer, pH 7.2 were added into a Eppendorf Protein LoBind®, 1.5 mL tubes and mixed well. The tube was placed into a magnetic stand to collect the beads against the side of the tube, and then the supernatant was discarded. This wash was repeated a total of 3 times. After that, 700 µL of lysate containing DYKDDDDK-tagged protein was added to the pre-washed magnetic agarose and inverted to mix, and the samples were incubated with mixing for 45 min at room temperature. The beads were collected using a magnetic stand, and the supernatant was discarded. The flow-through fraction was saved for subsequent downstream analysis. The beads with DYKDDDDK-tagged target proteins were washed twice with 500 µL of 10 mM PBS (pH 7.2) containing protease inhibitor and once with 500 µL of deionized water. A magnetic stand was used to collect the beads, and the supernatant was removed. Finally, the DYKDDDDK-tagged recombinant proteins were eluted from the beads by the acid elution method. 100 µL of IgG elution buffer, pH 2.8, with protease inhibitor was added to the tube, mixed well, and incubated for 5 min in SOP2 and for 12–15 min in SOP3 at room temperature with frequent vortexing. After incubation, the magnetic agarose was collected with a magnetic stand, and then

the supernatant that contained the eluted target protein was removed and kept in 1.5 mL microtubes. To neutralize the low pH, 15 µL of neutralization buffer (1 M Tris, pH 8.5) was added to the 100 µL of eluate immediately. The elution step was done three times for complete recovery of the abundant target. The process of optimizing the protocols, SOP1, 2 and 3 is illustrated in figure 1 and shown in supplementary table S1. The optimized protocol of SOP3 is described in supplementary.

The purified protein samples were aliquoted into small portions in Eppendorf Protein LoBind®, 1.5 mL tubes for further study. The concentration of all fractions including purified target proteins was analyzed by the Pierce™ BCA Assay. In addition, the percent recoveries for purified target proteins in total eluates were calculated by dividing the amount of purified target protein recovered (µg) by the amount of total crude proteins added and multiplying the results by 100.

Sodium Dodecyl Sulphate-Polyacrylamide Gel Electrophoresis (SDS-PAGE) and western blot

The purified protein abilities were detected using DYKDDDDK-tagged antibody (HRP) (Genscript), HLA-A and HLA-B purified MaxPab mouse polyclonal antibodies (Abnova) with the western blotting method. The working concentrations of crude and purified proteins were 10 µg/mL and 1 µg/mL, respectively, according to the manufacturer's protocol[14]. The proteins separated on a 12.5% sodium dodecyl sulfate polyacrylamide gel electrophoresis at 150 volts for 90 mins were electronically transferred onto polyvinylidene fluoride membranes (PVDF). The PVDF membranes were blocked with 5% skim milk in 0.1% TBS-T at RT for 1 h and then incubated with 0.5 µg/mL of anti-DYKDDDDK tag antibody (HRP) or anti-HLA-A and -B at 4 °C for 18 h. After incubation, the membranes were treated with 0.1% TBS-T for 3 times and probed with anti-HLA-A and -B were incubated with HRP-conjugated goat anti-mouse secondary antibodies (Biolegend) at RT for 1 h. The bands of protein were detected with the enhanced luminol-based chemiluminescent (ECL) western blotting substrate kit (Amersham™, GE Healthcare UK) according to the manufacturer's instructions and finally imaged with the chemiluminescent imaging system (Amersham Imager 600, Cytiva, USA). The outline of the designed experiment for three different protocols of protein purification is summarized in figure 2.

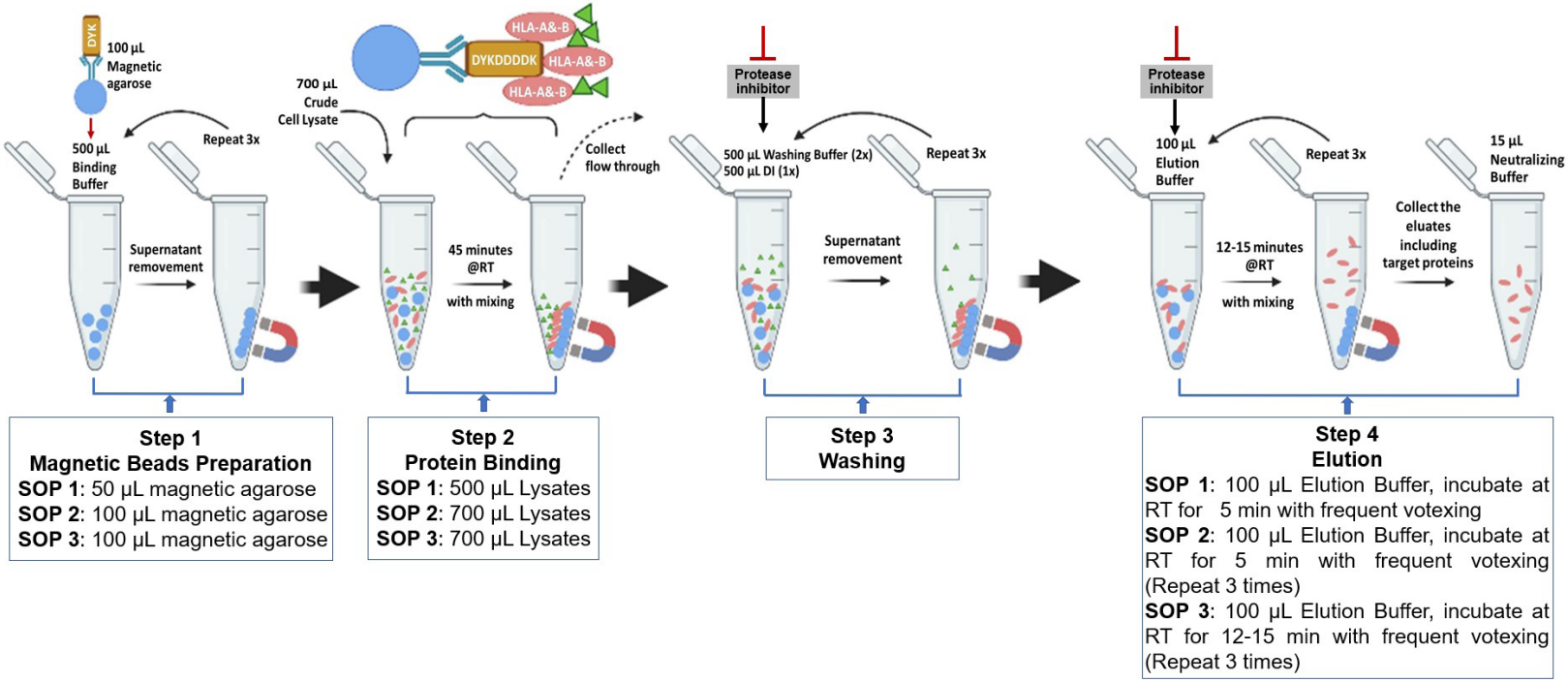

Figure 1 Schematic diagram of DYKDDDDK-tagged HLA-A and -B proteins purification protocol including the optimization steps. Three standard operating protocols were implemented as SOP1, SOP2, and SOP3. In the boxes for each step, the optimized factors for optimized protocols were shown.

Statistical Analysis

All experiments were carried out in triplicate if not stated otherwise in the figures. The purified protein concentrations in eluates were shown as the mean ± SD of three independent experiments. The statistical analysis was performed by using SPSS Statistics for Windows, version 19.0 (SPSS, Inc., Chicago, IL, USA). The distribution of the collected data in this study was tested by the Shapiro-Wilk test. Statistical significance was conventionally accepted when p-value < 0.05. One-way ANOVA with Tukey's test or independent student t-test (with normal distribution) was analyzed for eluate 1 (E1) and 2 (E2), respectively.

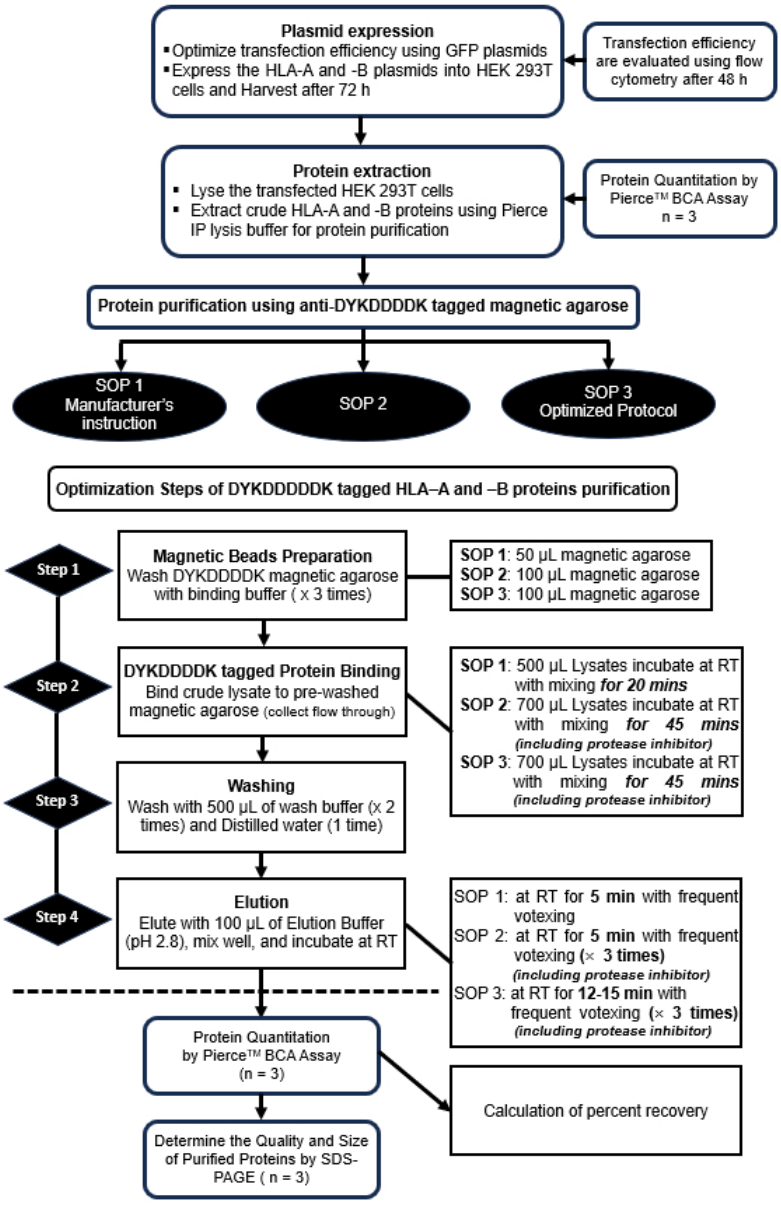

Figure 2 A workflow overview of three DYKDDDDK-tagged HLA-A and -B proteins purification protocols by Pierce™ anti-DYKDDDDK magnetic agarose kit.

Note: The optimized factors in each step for optimized protocols were shown; n indicates the number of technical triplicates used in this study.

Results

Optimization of transfection efficiency

To optimize the transfection efficiency, HEK 293T cells were transfected with 1 µg of GFP plasmid DNA per well with varying amounts of transfection reagent. The cells were collected 24 h after transfection, and the transfection efficiencies were evaluated by the flow cytometric method. The transfection efficiencies were 95.9%, 97.5%, 98.1%, and 97.2% at the different ratios of transfection reagent and plasmid, 1:1, 2:1, 3:1, and 4:1, respectively (Figure 3). The highest transfection efficiency was determined to be 98.1% at a 3:1 ratio of transfection reagent to GFP plasmid. This ratio was consistent with the recommended ratio by Roche Diagnostics GmbH, Germany[12]. It also had a similar efficiency rate of 97.5% at a 2:1 ratio of transfection reagent to GFP plasmid.

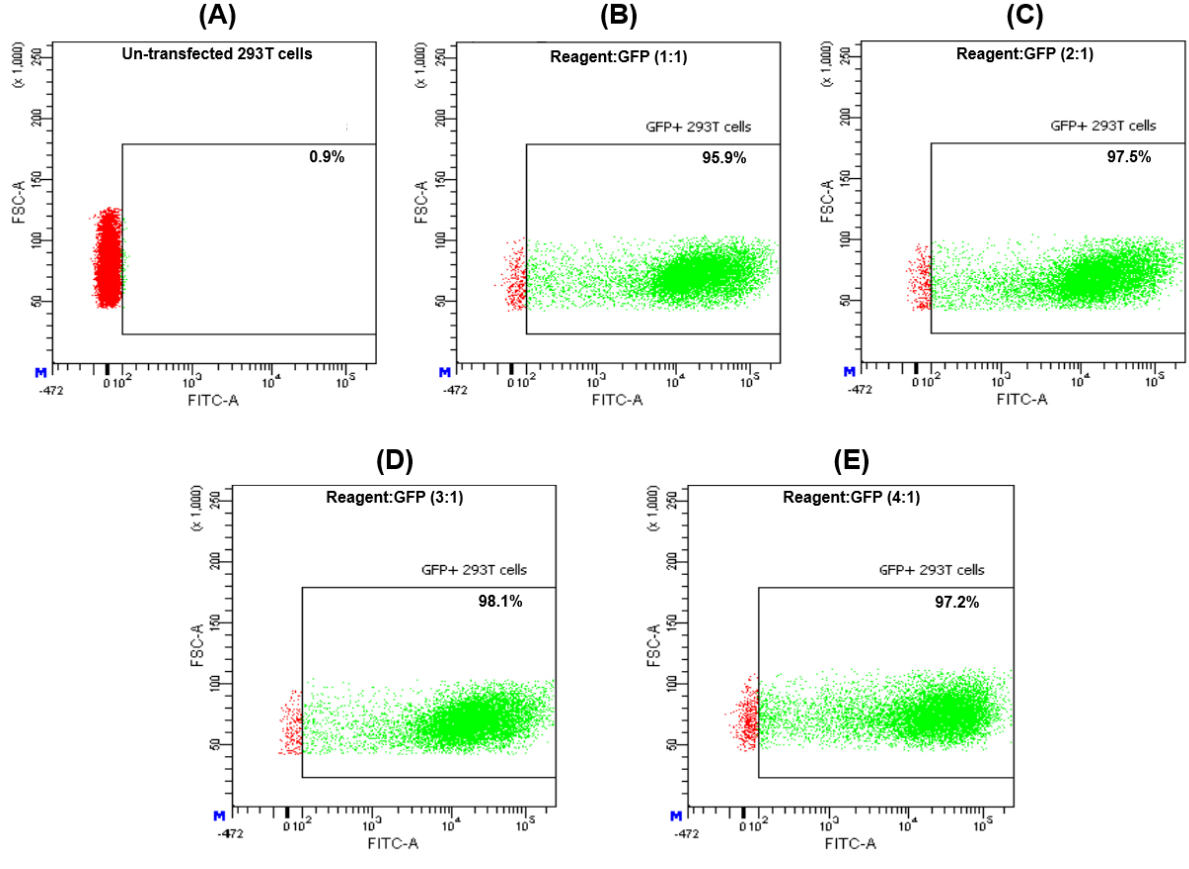

Figure 3 The optimization of transfection efficiency by using GFP plasmid DNA by flow cytometry (Scatter plots represented the flow cytometry analysis of transfectants) and HLA-A plasmid DNA by SDS-PAGE. (A) un-transfected HEK 293T as a negative control; the transfection regent and GFP plasmid ratios of 1:1, 2:1, 3:1, and 4:1 in (B), (C), (D), and (E), respectively.

Purified HLA-A and -B proteins concentration and percent recovery

The optimal conditions for protein expression and purification were used to produce large amounts of protein. The concentrations of HLA-A and -B proteins were very low in the eluates, 18 ± 11.96 µg/mL and 12 ± 8.32 µg/mL, respectively using SOP1 (Supplementary Table S2).

Then, both HLA-A and HLA-B proteins were produced, and purification was carried out using

an optimized protocol (SOP2). As shown in figure 4A and 4B, SOP2 considerably enhanced the quantities of isolated HLA-A and HLA-B proteins in E1 when compared to SOP1 (p-value = 0.017 for HLA-A and p-value = 0.008 for HLA-B).

Finally, the number of elution times and incubation times in the elution step condition were increased, and SOP3 was established to increase target protein yield. We found an average increase in purified protein yield in E1 and E2 of between 2- and 3-fold using SOP3 when compared with SOP2 (Supplementary Table S2). The statistical analysis indicated no significant difference in purified protein concentration in E1 between SOP2 and 3 of HLA-A (p-value = 0.335) and HLA-B (p-value = 0.244) (Figure 4A and 4B). Despite this, the protein concentration in E1 as determined by SOP1 and SOP3 showed highly significant differences, with p-value = 0.004 for HLA-A and p-value = 0.002 for HLA-B. Similarly, for purified HLA-A (p-value < 0.001) and HLA-B (p-value = 0.001), very significant differences in E2 were observed between SOP1 and SOP3 (Figure 4A and 4B).

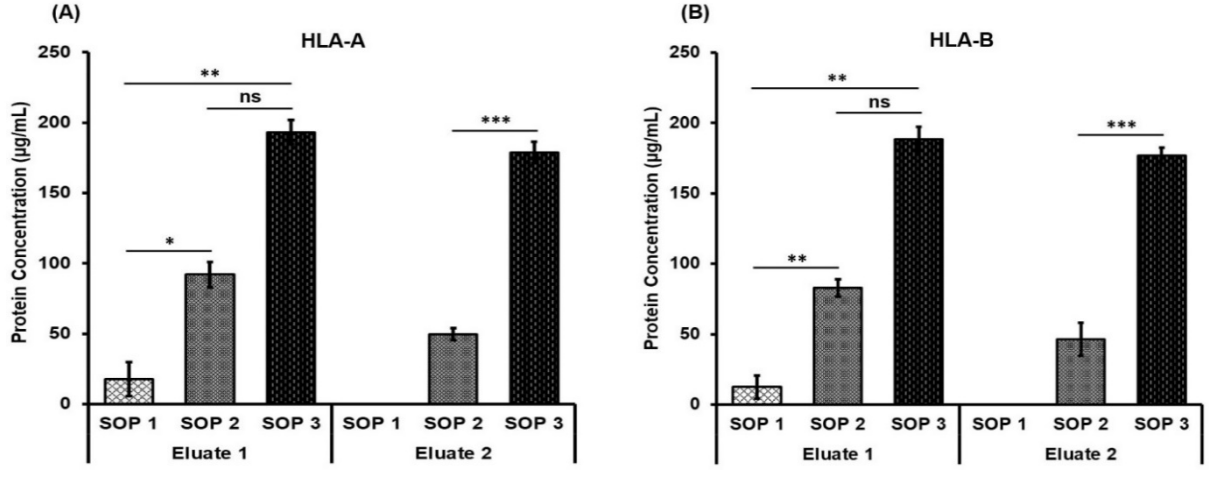

Figure 4 Comparison of purified protein concentrations amongst different SOPs.
Note: (A) Comparison of SOP1, SOP2, and SOP3 for purified HLA-A protein concentration in eluates 1 and 2. (B) Comparison of SOP1, SOP2, and SOP3 for purified HLA-B protein concentration in eluates 1 and 2. Each dataset illustrated the mean and standard deviation obtained from three independent experimental triplicates (ns = no significant, * p-value < 0.05, ** p-value < 0.01, *** p-value < 0.001).

In addition, the percent recoveries for purified target proteins in total eluates were calculated by dividing the amount of purified target protein recovered (µg) by the amount of total crude proteins added and multiplying the results by 100[15]. The percent recovery of HLA-A and -B proteins in E1 purified by SOP3 is remarkably higher than those obtained by SOP1 and SOP2 (Table 1). There were no statistically significant differences in the percent recovery of E1 between SOP1 and SOP2, as well as between SOP2 and SOP3, for both purified proteins (p-value > 0.05). Although the percent recovery of E1 for HLA-A between SOP1 and 3 was statistically significant (p-value = 0.018), there was no significant difference for HLA-B (p-value = 0.093) (Supplementary Figure S2A). It was interesting to note that the purified HLA-A and HLA-B proteins in total eluates had percent recoveries of 81.15% and 80.73%, respectively, using SOP3 (Table 1). Moreover, the statistical analysis revealed highly significant differences in the total eluates of HLA-A (p-value = 0.005) and HLA-B (p-value = 0.001) by SOP3 compared to that of SOP2 (Supplementary Figure S2B).

Table 1 Percent recoveries of purified HLA-A and -B proteins using different SOPs

Proteins amount in Total Eluates	HLA-A (% Recovery)				HLA-B (% Recovery)			
	SOP1	SOP2	SOP3	*p*-value	SOP1	SOP2	SOP3	*p*-value
E1 [C (µg)]	13.48 ± 9.14	21.88 ± 5.98	42.18 ± 2.99	0.018	15.11 ± 12.3	24.13 ± 3.40	41.72 ± 4.57	0.093
E1+E2 [C (µg)]	ND*	33.71 ± 9.52	81.15 ± 3.62	0.005	ND*	37.5 ± 3.95	80.73 ± 7.33	0.001

Note: ND*, not done.

Evaluation of the quality of purified HLA-A and -B proteins by SDS-PAGE and western blot analysis

The quality and size of purified HLA-A and -B proteins were assessed using SDS-PAGE and western blot analysis. By using SOP1, the bands were not seen in elutes even though the thick bands were observed at 52 kDa in accordance with the predicted size of the Genscript company in crude lysates and flowthrough fractions of both proteins against anti-HLA-A and -B antibodies (Figure 5A and 5B). Moreover, the thick bands were detected at 52 kDa of HLA-A and -B proteins when probed with DYKDDDDK tag antibody (HRP) (Figure 5C).

When protein purification was carried out using the optimized protocol (SOP2) (Supplementary Table S1), the more-intense single bands in E1 for both HLA proteins were observed compared to SOP1. The weak single bands were found in E2, while no band was seen in eluates 3 (E3) of SOP2 for isolated HLA-A and -B (Figure 5D and 5E).

The 2x sample buffer containing DTT was directly added to the beads to test the target proteins on the beads. The mixture was incubated for 5 min at 100 °C before being spun down. Next, the magnetic beads were collected in a magnetic stand, and the supernatants were used for the SDS-PAGE and western blotting. The target proteins were found to be thick bands in the supernatants of both proteins suggesting that they were not fully eluted from the beads (Figure 5F).

After purification using a modified elution step condition (SOP3) (Supplementary Table S1), the single thick bands were detected in E1 and E2 of both purified DYKDDDDK-tagged HLA-A and -B proteins (Figure 5G and 5H). Nonetheless, no bands were detected in E3 in all experiments using SOP2 and 3. It could be due to denaturation of the target purified proteins. These findings revealed that the first repeated elution steps were covered only for complete recovery of highly abundant targets.

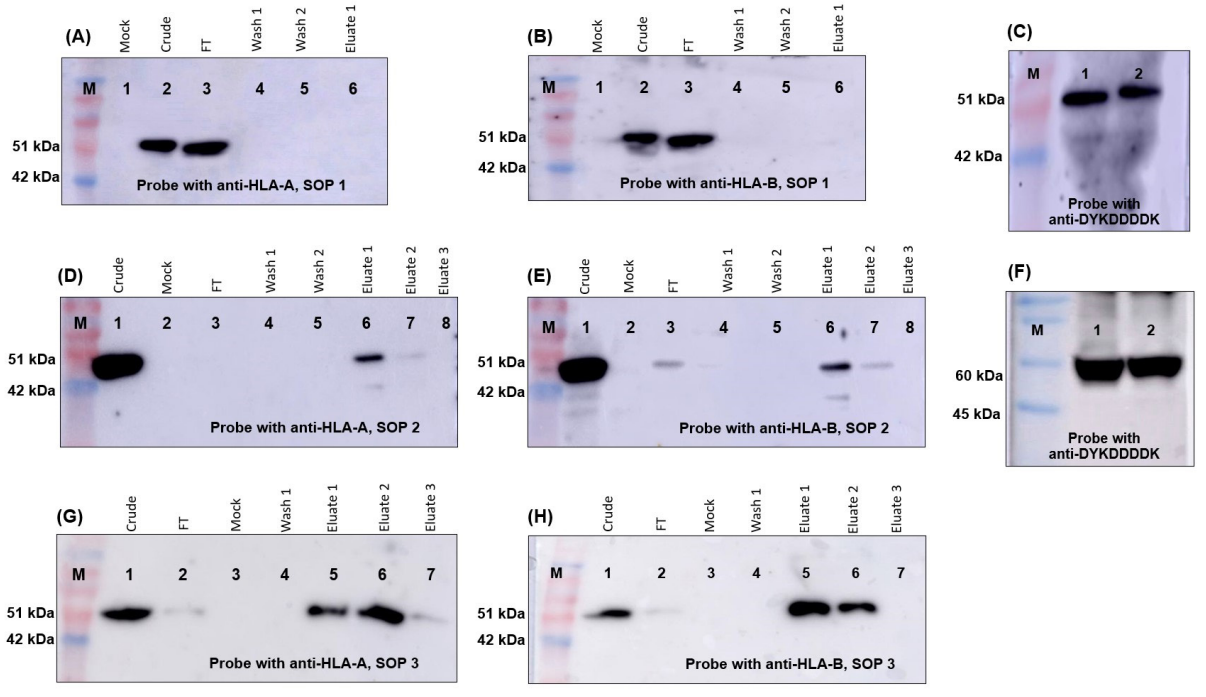

Figure 5 The quality evaluation of purified proteins by SDS-PAGE and western blot analysis.
Note: (A) and (B) Purified HLA-A and -B proteins by probing with specific HLA-A and -B antibodies, respectively. (C) Crude lysates by probing with DYKDDDDK tag antibody (HRP). Lane M, Protein Marker; Lane 1, Crude lysate of HLA-A; Lane 2, Crude lysate of HLA-B. (D) and (E) Crude lysates and purified HLA-A and -B proteins by probing with specific HLA-A and -B antibodies, respectively. (F) Checking the elution steps using the sample directly removed from saved magnetic beads used for purification by probing with DYKDDDDK tag antibody (HRP). Lane M, Protein marker; Lane 1 and 2: Sample from the beads that was used for HLA-A and -B proteins purification, respectively. (G) and (H) Crude lysates and purified HLA-A and -B proteins by probing with specific HLA-A and -B antibodies, respectively.

Discussion

Protein structural and functional information is frequently required in large quantities and at high purity for the purpose of developing a new biomolecular technique. The low efficiency levels of exogenous protein expression and purification are frequently encountered in order to obtain sufficient amounts of native protein[16]. The human embryonic kidney 293 (HEK 293) cell is one of the most commonly used mammalian cell lines in research platforms for protein production[17]. The HEK 293T cells are originated from HEK 293 cells along with the SV40 large T antigen, which can bind to SV40 enhancers of expression vectors and stably express to improve protein production[18].

In this study, GFP plasmid was transfected into the HEK 293T cell line by using the X-treme GENE HP DNA transfection reagent. The transfection efficiency was systematically optimized using GFP and evaluated by flow cytometry. Our results on GFP plasmid showed that the transfection efficiencies achieved under these optimized conditions had a high expression level. Although the highest percentage of transfection efficiency was 98.1% at a 3:1 ratio of transfection reagent to plasmid, the transfection percentage (97.5%) was similar at a 2:1 ratio of transfection reagent to plasmid. Therefore, the optimal transfection condition was determined as a 2:1 ratio of transfection reagent and plasmid in our study. Lipofection

systems utilizing the X-treme Gene HP DNA transfection reagent and the HEK 293T cell line were effective in achieving high expression of HLA-A and HLA-B genes in the pcDNA3.1+/C-(K)-DYK vector.

Another important facet and the main objective of this study is to optimize the purification method using the anti-DYKDDDDK magnetic agarose system for isolating the recombinant HLA-A and -B proteins from crude cell lysates. The development of universal purification and capture strategies for native proteins has been challenging due to the diversity of proteins and their biochemical properties[19]. The small epitope tags, such as the DYKDDDDK (FLAG), c-Myc, and HA tags, which have a short amino acid sequence attached to the N- or C-terminus of a recombinant protein, are able to strongly and precisely bind their respective immunoaffinity resins[20,21]. Magnetic resins can purify the affinity-tagged protein without multiple centrifugation steps. Moreover, magnetic nanoparticles (MNPs) can be reused due to their superparamagnetic capability; consequently, it can reduce the high cost of conventional protein purification methods such as chromatography, centrifugation, and membrane separation and their turn-around times[10].

In this work, the Pierce™ Anti-DYKDDDDK Magnetic Agarose system was used to purify the DYKDDDDK-tagged recombinant HLA-A and -B proteins. A high-affinity rat monoclonal antibody (clone L5) covalently attaches to a magnetite-embedded agarose core particle by recognizing the small amino acid sequence, DYKDDDDK. The Pierce™ Anti-DYKDDDDK Magnetic Agarose recognizes the DYKDDDDK-tagged proteins with the tag on either the N- or C-terminus[13]. At the beginning, to purify crude lysates, we applied the manufacturer's protocol, represented as SOP1. Unfortunately, the C-terminally DYKDDDDK-tagged HLA-A and -B proteins were not purified successfully. The purified protein concentrations were very low in the eluates of HLA-A and -B, and no bands were identified in the eluates in the SDS-PAGE profile. The possible cause is that all target proteins cannot bind to the magnetic beads adequately. It depends on the ratio of magnetic agarose slurry to crude lysate volume for sufficient binding of antigen and antibody. In addition, the target proteins did not elute from the beads. Therefore, SOP2 was established, which significantly boosted the concentrations of purified proteins in total eluates for HLA-A and -B. These concentrations were not enough for use in further studies. In addition, SDS-PAGE and western blot analysis revealed an indistinct band in E2 and a blank in E3. In this condition, the DYKDDDDK-tagged proteins could not be eluted from the beads, although most of the target proteins were bound to the magnetic beads. In this case, the target proteins were found to be thick bands in the supernatants of both proteins. According to this finding, most of the target proteins could bind to the magnetic beads. We identified two potential causes for these issues. In this work, the acid elution protocol was applied using a commercial IgG elution buffer at pH 2.8. The first reason was that the elution conditions were too mild, and the second reason was that purified proteins in those eluates were degraded because a strong acid buffer was used in the elution step even though we added the neutralizing buffer, 1 M Tris, at pH 8.5 immediately. Therefore, the elution condition was optimized to a more stringent method in which the incubation time of the elution step was increased to 12–15 min, ensuring that 15 min was not exceeded to avoid the captured antibodies leaching from the beads. Moreover, the protease inhibitor was also added to the washing buffer and elution buffer to prevent the degradation of target proteins. The repeated elution step was performed three times as SOP2 to obtain the highly purified protein yield. The pH of a protein solution influences the success of protein crystallization[22]. In addition, in order to maximize stability, the pH of the storage buffer should be at least one unit away from the pI values of the target protein[23]. In this study, the pI values of the produced DYKDDDDK-tagged HLA-A

and -B proteins were 6.09 and 5.57, respectively. Therefore, the pH of the elution buffer was adjusted by adding neutralizing buffer at 7.2. Finally, we could successfully set up a reliable and functionally optimized protocol, represented as SOP3, for the purification of the DYKDDDDK-tagged HLA-A and -B proteins with a high yield concentration (170–200 µg/mL).

Furthermore, the overall percentage recovery of purified HLA-A (81.15%) and -B proteins (80.73%) in total eluates obtained by SOP3 was significantly higher than those obtained by SOP1 and 2. Therefore, this study improved the effectiveness of the protocol for recombinant HLA protein purification by using an anti-DYKDDDDK magnetic agarose system.

There is no study of the purification method of DYKDDDDK-tagged recombinant HLA-A and -B proteins using the commercial kit, the Pierce™ anti-DYKDDDDK magnetic agarose system in the laboratory practice. Although the selected purification kit was used according to its manual, DYKDDDDK-tagged recombinant HLA-A and -B proteins were not successfully purified. In practice, we encountered many factors that influenced the purification of DYKDDDDK-tagged recombinant HLA-A and -B proteins using the Pierce™ anti-DYKDDDDK magnetic agarose method. We verified the crucial factors in each step of protein purification, including the magnetic agarose slurry volume (100 µL), crude lysate volume (700 µL), the incubation time for DYKDDDDK-tagged protein binding to pre-washed magnetic agarose beads (45 min), the elution step (3 times), increased the incubation time in the elution step (12–15 min) and added the protease inhibitor to the washing buffer and elution buffer.

In this study, the potential of the Pierce™ anti-DYKDDDDK magnetic agarose kit with an improved and reliable protocol was evaluated to purify the DYKDDDDK-tagged recombinant HLA-A and -B proteins. The purified HLA-A and -B proteins obtained using this improved, reliable protocol have been successfully applied in the establishment of an ion-sensitive field-effect transistor-based immunosensor for the detection of relevant anti-HLA antibodies, especially in the field of kidney transplantation[24]. Furthermore, this improved protocol would become an important tool that could provide a valuable guideline for the production and purification of other DYKDDDDK-tagged recombinant proteins.

Conclusion

For protein production, the X-treme GENE HP DNA transfection reagent was used to transfect HEK 293T cells with HLA-A and HLA-B inserted pcDNA3.1+/C-(K)-DYK plasmids. The transfection conditions were optimized using the plasmid encoding green fluorescent protein, reporting on conditions that would ensure optimal expression. In this study, we explored and evaluated the critical factors at each step of the purification process. In summary, an improved and functional protocol of the Pierce™ Anti-DYKDDDDK Magnetic Agarose system was introduced in the DYKDDDDK-tagged recombinant HLA-A and -B protein purification, increasing the percent recovery of the purified high yield proteins that can be used *in vitro* studies.

Take home messages

An improved and functional protocol of the Pierce™ Anti-DYKDDDDK Magnetic Agarose system was introduced in the DYKDDDDK-tagged recombinant HLA-A and -B protein purification, increasing the percent recovery of the purified high yield proteins that could provide a useful guideline for the purification of other DYKDDDK-tagged recombinant proteins.

Conflicts of interest

The authors declare no conflict of interest.

Acknowledgements

We gratefully acknowledge financial support from the Centre for Research and Development of Medical Diagnostic Laboratories (CMDL), Faculty of Associated Medical Sciences, Khon Kaen University, Thailand and the Khon Kaen University Scholarship for ASEAN and GMS Countries' Personnel, 2017.

References

1. Klein JAN, Sato A. The HLA system: First of two parts. N Engl J Med 2000; 343(10): 702–9.
2. Williams TM. Human leukocyte antigen gene polymorphism and the histocompatibility laboratory. J Mol Diagn 2001; 3(3): 98–104.
3. Puttarajappa C, Shapiro R, Tan HP. Antibody-Mediated Rejection in Kidney Transplantation: A Review. J Transplant 2012; 2012: 1–9.
4. Lefaucheur C, Loupy A, Hill GS, Andrade J, Nochy D, Antoine C, et al. Preexisting donor-specific HLA antibodies predict outcome in kidney transplantation. J Am Soc Nephrol 2010; 21(8): 1398–407.
5. Roux A, Bendib Le Lan I, Holifanjaniaina S, Thomas KA, Hamid AM, Picard C, et al. Antibody-Mediated Rejection in Lung Transplantation: Clinical Outcomes and Donor-Specific Antibody Characteristics. Am J Transplant 2016; 16(4): 1216–28.
6. Zhang J, Qi L, Zheng WT, Tian Y Le, Chi AP, Zhang ZQ. Novel functionalized poly(glycidyl methacrylate-co-ethylene dimethacrylate) microspheres for the solid-phase extraction of glycopeptides/glycoproteins. J Sep Sci 2017; 40(5): 1107–14.
7. Ma Y, Chen T, Iqbal MZ, Yang F, Hampp N, Wu A, et al. Applications of magnetic materials separation in biological nanomedicine. Electrophoresis 2019; 40(16): 2011–28.
8. Thekkilaveedu S, Krishnaswami V, Mohanan DP, Alagarsamy S, Natesan S, Kandasamy R. Lactic acid-mediated isolation of alpha-, beta- and kappa-casein fractions by isoelectric precipitation coupled with cold extraction from defatted cow milk. Int J Dairy Technol 2020; 73(1): 31–9.
9. Dias AMGC, Hussain A, Marcos AS, Roque ACA. A biotechnological perspective on the application of iron oxide magnetic colloids modified with polysaccharides. Biotechnol Adv 2011; 29(1):142–55.
10. Borlido L, Azevedo AM, Roque ACA, Aires-Barros MR. Magnetic separations in biotechnology. Biotechnol Adv 2013; 31(8):1 374–85.
11. Liu S, Yu B, Wang S, Shen Y, Cong H. Preparation, surface functionalization and application of Fe3O4 magnetic nanoparticles. Adv Colloid Interface Sci 2020; 281: 102165.
12. Roche Diagrnostics. X-tremeGENE HP DNA Transfection Reagent [online] 2020 [cited 2023 April 27] Available from https://www.sigmaaldrich.com/deepweb/assets/sigmaaldrich/product/ documents/234/408/xtghp-ro.pdf
13. A CN. Pierce TM Anti-DYKDDDDK Magnetic Agarose [online] 2017 [cited 2023 April 27] Available from https://assets.fishersci.com/TFS-Assets/LSG/manuals/MAN0017395_2162708_PierceAnti_DYKDDDDK_MagAgarose_PI.pdf
14. Antibody DT. GenEZ TM ORF clone User manual [online] 2015 [cited 2023 April 27] Availabel from https://www.genscript.com/gsfiles/User%20manual_GenEZ%20ORF% 20Clone%20Products.pdf
15. Moore DD. Current Protocol in Molecular Biology. In: Ausubel FM, Brent R, Kingston RE, Moore DD, Seidman JG, Smith JA, Struhl K, editors. New Jersey: John Wiley & Sons, Inc; 2006. p. 4412–35.
16. Halff EF, Versteeg M, Brondijk THC, Huizinga EG. When less becomes more: Optimization of protein expression in HEK293-EBNA1 cells using plasmid titration - A case study for NLRs. Protein Expr Purif 2014; 99: 27–34.
17. Melville M, Estes S. Mammalian Cell Line Developments in Speed and Efficiency. Adv Biochem Eng Biotechnol 2013; 123(July 2015): 127–41.

18. DuBridge RB, Tang P, Hsia HC, Leong PM, Miller JH, Calos MP. Analysis of mutation in human cells by using an Epstein-Barr virus shuttle system. Mol Cell Biol 1987; 7(1): 379–87.
19. Pina AS, Lowe CR, Roque ACA. Challenges and opportunities in the purification of recombinant tagged proteins. Biotechnol Adv 2014; 32(2): 366–81.
20. Nilsson J, Ståhl S, Lundeberg J, Uhlén M, Nygren PÅ. Affinity fusion strategies for detection, purification, and immobilization of recombinant proteins. Protein Expr Purif 1997; 11(1): 1–16.
21. Fritze CE, Anderson TR. Epitope tagging: General method for tracking recombinant proteins. Methods Enzymol 2000; 327(1987): 3–16.
22. Judge RA, Jacobs RS, Frazier T, Snell EH, Pusey ML. The effect of temperature and solution pH on the nucleation of tetragonal lysozyme crystals. Biophys J 1999; 77(3): 1585–93.
23. Alberti S, Saha S, Woodruff JB, Franzmann TM, Wang J, Hyman AA. A User's Guide for Phase Separation Assays with Purified Proteins. J Mol Biol 2018; 430(23): 4806–20.
24. Min TZMMM, Phanabamrung S, Chaisriratanakul W, Pankiew A, Srisuwan A, Chauyrod K, et al. Biosensors Based on Ion-Sensitive Field-Effect Transistors for HLA and MICA Antibody Detection in Kidney Transplantation. Molecules 2022; 27(19): 1–18.

Supplementary

Table S Comparison of concentrations of HLA-A and -B proteins between SOP 1, 2 and 3

Steps of purification	HLA-A (µg/mL)			HLA-B (µg/mL)		
	SOP 1	SOP 2	SOP 3	SOP 1	SOP 2	SOP 3
Crude lysate	2014 ± 46.30	2058 ± 76.38	2051 ± 37.61	1931 ± 43.45	1949 ± 112.11	1965 ± 34.30
Flow through	1676 ± 52.50	1481 ± 17.32	1436 ± 36.31	1720 ± 40.65	1459 ± 42.72	1351 ± 40.23
Wash fraction	103 ± 13.92	104 ± 20.05	112 ± 12.99	95 ± 13.92	113 ± 20.46	104 ± 12.33
Wash fraction	30 ± 10.25	36 ± 26.73	45 ± 13.23	24 ± 10.41	30 ± 15.21	57 ± 14.08
Eluate 1	18 ± 11.96	92 ± 9.01	193 ± 8.45	12 ± 8.32	83 ± 6.29	189 ± 8.73
Eluate 2	ND*	50 ± 4.33	179 ± 7.52	ND*	46 ± 11.81	177 ± 5.94
Eluate 3	ND*	35 ± 2.89	49 ± 10.90	ND*	31 ± 6.29	49 ± 4.33

Note: ND* = Not Done

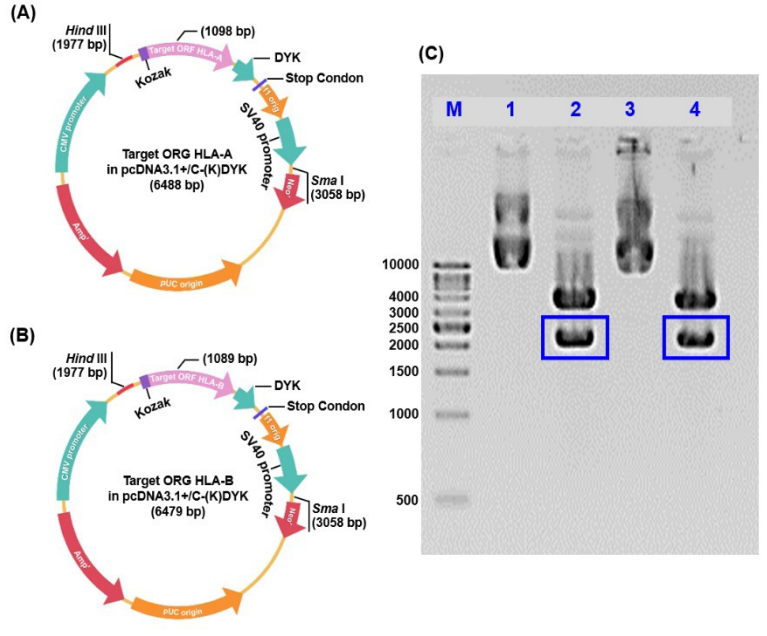

Figure S1 The illustration of HLA-A and -B plasmids and the restriction enzyme analysis.
Note: (A and B) Schematic representation of the pcDNA3.1$^+$/C-(K)-DYK vector map with target ORF HLA-A with (6488 bp) and -B gene (6479 bp). (C) Restriction digestion of HLA-A and -B/pcDNA3.1$^+$/C-(K)-DYK with *Hind*III and *Sma*I. Lane M: DNA Ladder. Lane 1 and 3: The undigested clones, HLA-A and -B DNA clones showing the bands of 6488 bp and 6479 bp represent the full size of plasmid, respectively. Lane 2 and 4: After digestion with *Hind*III and *Sma*I, the bands at 4400 and 2000 bp in the blue boxes indicate the inserted target HLA-A and -B genes.

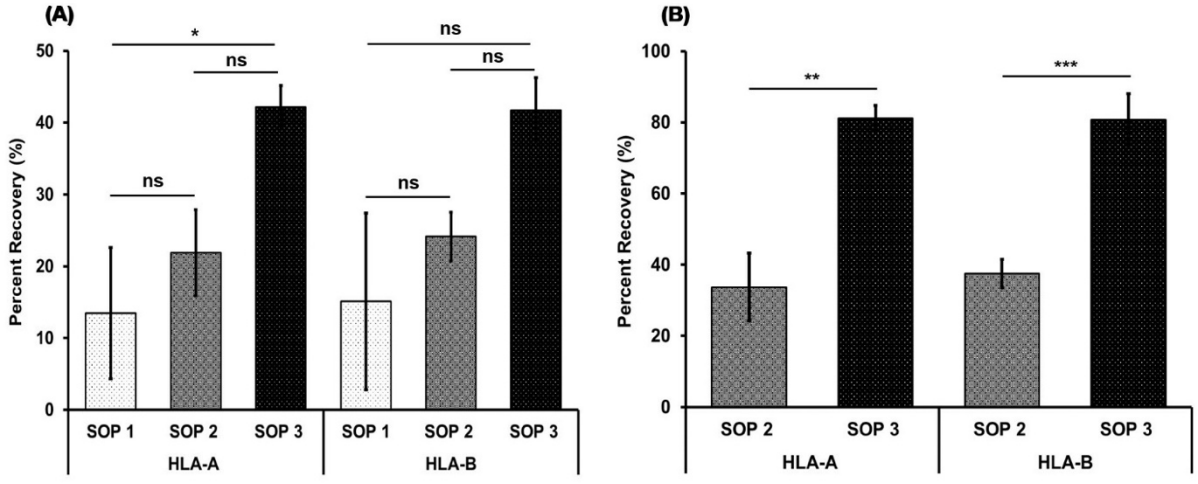

Figure S2 The percent recovery of each SOPs for purified HLA-A and -B proteins.

Note: (A) The percent recovery of purified HLA-A and -B proteins in eluate 1 by SOP 1, 2 and 3. (B) The percent recovery of purified HLA-A and -B proteins in total eluates (Eluates 1 and 2) by SOP 2 and 3. Each dataset illustrated the mean and standard deviation obtained from three independent experimental triplicates. (ns = no significant, * p-value < 0.05, ** p-value < 0.01, *** p-value < 0.001).

1. HLA-A and HLA-B cDNA ORF clones

HLA-A cDNA ORF clones (Product ID-OHu29153)
(NCBI Ref.Seq: NP_001229687.1) _ HLA-A*01:01

MAVMAPRTLLLLLSGALALTQTWAGSHSMRYFFTSVSRPGRGEPRFIAVGYVDDTQFVRFDSDAASQKMEPRAPWIEQEG
PEYWDQETRNMKAHSQTDRANLGTLRGYYNQSEDGSHTIQIMYGCDVGPDGRFLRGYRQDAYDGKDYIALNEDLR
SWTAADMAAQITKRKWEAVHAAEQRRVYLEGRCVDGLRRYLENGKETLQRTDPPKTHMTHHPISDHEATLRCWALG
FYPAEITLTWQRDGEDQTQDTELVETRPAGDGTFQKWAAVVVPSGEEQRYTCHVQHEGLPKPLTLRWELSSQPTIPIVGI
IAGLVLLGAVITGAVVAAVMWRRKSSDRKGGSYTQAASSDSAQGSDVSLTACKV

HLA-B cDNA ORF clones (Product ID-OHu26926D)
(NCBI Ref.Seq: NM_005514.6) _ HLA-B*07:02

MLVMAPRTVLLLLSAALALTETWAGSHSMRYFYTSVSRPGRGEPRFISVGYVDDTQFVRFDSDAASPREEPRAPWIEQEG
PEYWDRNTQIYKAQAQTDRESLRNLRGYYNQSEAGSHTLQSMYGCDVGPDGRLLRGHDQYAYDGKDYIALNEDLR
SWTAADTAAQITQRKWEAAREAEQRRAYLEGECVEWLRRYLENGKDKLERADPPKTHVTHHPISDHEATLRCWALG
FYPAEITLTWQRDGEDQTQDTELVETRPAGDRTFQKWAAVVVPSGEEQRYTCHVQHEGLPKPLTLRWEPSSQSTVPIV
GIVAGLAVLAVVVIGAVVAAVMCRRKSSGGKGGSYSQAACSDSAQGSDVSLTA

ORIGINAL ARTICLE

Arch AHS

Archives of Allied Health Sciences 2023; 35(3): 39-47.

Effect of paraquat on red blood cell oxidative stress in individuals with hemoglobin E trait and G6PD deficiency

Nattaphol Prakobkaew[1], Natthapak Sillawatthumrong[2], Supaporn Khamchan[2,3], Surachat Buddhisa[1,3*]

[1] Faculty of Allied Health Sciences, Burapha University, Chonburi, Thailand.
[2] Department of Medical Technology, School of Allied Health Sciences, University of Phayao, Phayao, Thailand.
[3] Unit of Excellence in Cellular and Molecular Immunodiagnosis and Therapy, School of Allied Health Sciences, University of Phayao, Phayao, Thailand.

KEYWORDS
Paraquat;
Oxidative stress;
G6PD deficiency;
Hemoglobin E trait.

ABSTRACT

Paraquat is one of the most widely used herbicides globally and is a potent inducer of cellular reactive oxygen species, which cause damage to cells and organs in humans and animals. Recently, paraquat was found to affect normal human and animal red blood cells (RBCs). However, the effects of paraquat on hemoglobin E (Hb E) and glucose-6-phosphate dehydrogenase (G6PD) deficiency, commonly observed in Thailand, are unknown. This study investigated the effects of paraquat on oxidative stress and osmotic fragility in RBCs of individuals with Hb E trait and G6PD deficiency *in vitro*. The RBCs of individuals with Hb E trait and G6PD deficiency and normal controls were exposed to pure or commercially available paraquat dichloride; malondialdehyde (MDA) levels and the osmotic fragility were evaluated after coculture for 24 hours. In all groups, RBCs exposed to paraquat had significantly increased MDA levels compared with those exposed to saline solution (controls). The MDA level of RBCs from individuals with Hb E trait was significantly higher than that of RBCs from normal controls. Furthermore, the initial hemolysis of saline- and paraquat-treated RBCs from individuals with Hb E trait and G6PD deficiency was significantly higher than that of RBCs from normal controls. These data suggest that paraquat induces increased lipid peroxidation in RBCs of individuals with Hb E trait and G6PD deficiency and that RBCs of individuals with Hb E trait and G6PD are slightly more fragile than RBCs from normal individuals; however, paraquat does not affect the osmotic fragility of RBCs.

***Corresponding author:** Surachat Buddhisa, MT, PhD. Faculty of Allied Health Sciences, Burapha University, Chonburi, Thailand.
Email address: surachat.bu@buu.ac.th
Received: 3 August 2023/ Revised: 19 September 2023/ Accepted: 23 October 2023

Introduction

Paraquat is a toxic chemical widely used in agriculture as an herbicide for weed and grass control. Extensive paraquat applications and long-term exposure lead to widespread residues in soil, aquatic environments[1], plants, and food grains[2]. Paraquat has been found in both surface water and groundwater; in such environments, it is adsorbed onto particles and sediment and has a half-life between 2 and 820 years[3]. Paraquat has a strong affinity for soil particles and tends to remain in the soil for up to 20 years[4]. Moreover, it can be absorbed from the soil and transferred to agricultural products[2,4] that ultimately enter the food chain[1]. Paraquat can harm the neurological system and lead to dysfunction in the kidneys, liver, heart, lungs, and hematological system in humans and animals through the extensive generation of reactive oxygen species (ROS). Recently, studies in mice have shown that paraquat can induce transient anemia resulting from ROS production, which randomly eliminates young and mature circulating red blood cells (RBCs) and depresses erythropoietic activity in the bone marrow[5-9].

Hemoglobin E (Hb E) trait and glucose-6-phosphate dehydrogenase (G6PD) deficiency are common hemoglobinopathy and enzymopathy in countries in Southeast Asia, including Thailand[10]. Individuals with Hb E trait have higher antioxidant status because of a compensatory antioxidant response brought on by an excessive amount of oxidative stress, which lowers their antioxidant capacity[11]. G6PD deficiency is a human enzymopathy caused by inherited mutations of the X-linked gene *G6PD* that affect the ability of RBCs to respond to oxidative stress, thus making them susceptible to hemolysis. Previous studies have demonstrated that RBCs from individuals with Hb E and G6PD deficiency exhibit increased lipid peroxidation, increased activity of superoxide dismutase and decreased thiol glutathione (GSH) activity at baseline, and red blood cell defects may render RBC more susceptible to oxidative stress[12-14]. Paraquat was expected to increase RBC lipid peroxidation, which would lead to more rigid *RBCs in* individuals with Hb E and G6PD deficiency. In this study, we investigated the effects of paraquat on oxidative stress and osmotic fragility in RBCs of individuals with Hb E trait and G6PD deficiency subjects *in vitro*. Our findings could be useful in educating the public on the possible effects of this herbicide on human health, thereby reducing the negative effects of paraquat.

Materials and methods

Human subjects and blood samples

This study was approved by the Burapha University Ethics Committee for Human Research (Sci 046/2562). All participants provided informed consent. A total of 18 participants-10 healthy individuals, four individuals with G6PD deficiency, and four individuals with Hb E trait-were enrolled in this study. Individuals with underlying diseases, anemia, or taking antioxidant supplements including vitamin C, glutathione, and coenzyme Q10 were excluded. Whole blood (6 mL) was collected; 3 mL was added to lithium-heparin tubes and 3 mL was added to ethylenediaminetetraacetic acid (EDTA) tubes. EDTA blood samples were analyzed for complete blood count (CBC) by an automated hematology analyzer (Mindray BC-5800, Shenzhen, China); screened for thalassemia with one-tube osmotic fragility (OF) and dichlorophenol-indophenol precipitation (DCIP) tests; Hb typing was performed by cellulose acetate electrophoresis, and G6PD deficiency was assessed with fluorescent spot (FST) testing.

Thalassemia screening and hemoglobin typing

Screening for α-thalassemia, β-thalassemia, and Hb E was carried out with the KKU-OF and KKU-DCIP reagent kits (PCL Holding, Thailand) according to the manufacturer's instructions as described previously[15]. Both tests are interpreted with a negative and a positive control. The Hb types were determined by cellulose acetate electrophoresis (Helena Laboratories, Beaumont,

TX, USA). A_2A type Hb with a normal A_2 level (< 3.5%) was used for comparative interpretation. The samples were classified as normal (negative for KKU-OF and KKU-DCIP, A_2A pattern Hb typing) or Hb E trait (negative for KKU-OF, positive for KKU-DCIP, and EA pattern Hb typing).

Fluorescent spot test (FST) for screening of G6PD deficiency

A commercial FST kit (Trinity Biotech) was used to test for G6PD deficiency. The FST test was performed according to the manufacturer's instructions, as described elsewhere[16]. The samples were divided into three groups: normal (strong fluorescence at 5 and 10 minutes); intermediate (poor fluorescence at 5 minutes and moderate fluorescence at 10 minutes); and deficient (no fluorescence at 5 or 10 minutes).

Red blood cell culture

Lithium-heparinized blood samples were centrifuged at 3,000 rpm for 5 minutes. The plasma and buffy coat were removed, and the samples were washed twice with 0.85% saline solution; subsequently, 1 mL of packed RBCs was resuspended in 2 mL of 0.85% saline solution. The RBC count was determined by an automated hematology analyzer. RBCs (1×10^9/mL) were exposed to either 0.85% saline solution as a negative control or paraquat dichloride, either pure (Sigma-Aldrich) or commercially available, at final concentrations of 100 and 200 ug/mL for 24 hours at 37 °C in 5% CO_2.

Determination of malondialdehyde level by thiobarbituric acid reactive substances assay

The MDA levels were measured by using thiobarbituric acid reactive substances (TBARS) assay modified from Klarod et al[17]. A 25 µL of 0.1 mM butylated hydroxyl toluene (Sigma-Aldrich), 250 µL of 5 mM ethylenediamine tetraacetic acid (Sigma-Aldrich), 500 µL of 8.1% (w/v) sodium dodecyl sulfate (Sigma-Aldrich), 500 µL of 10% (w/v) trichloroacetic acid, and 750 µL of 0.67% (w/v) thiobarbituric acid were added to 500 µL of culture supernatant and standard malondialdehyde (MDA) solution. The mixture was heated in a boiling water bath at 95 °C for 30 minutes before being placed in water for 10 minutes. After cooling, the mixture was centrifuged at 3,000 rpm for 15 minutes, and the supernatant was transferred to a flat-bottom plate. The absorbance was measured at 532 nm with microplate reader (Molecular Devices, CA, USA)[17]. Each standard MDA solution and sample was tested in duplicate, and if the measurement values differed by more than 10%, the test was repeated. MDA standard solution was prepared using 1,1,3,3 tetramethoxypropane (Sigma-Aldrich) as the standard. The results were expressed as nM MDA.

Determination of erythrocyte osmotic fragility

RBCs (1×10^9/mL) from whole blood in lithium-heparin were treated with either a 0.85% saline solution or commercially available paraquat (cPQ) at a final concentration of 200 ug/mL at 37 °C in 5% CO_2 for 24 hours. Erythrocyte osmotic fragility (EOF) was assessed by adding 20 µL of treated RBCs to a set of test tubes containing 1.00%, 0.85%, 0.75%, 0.60%, 0.55%, 0.50%, 0.45%, 0.40%, 0.35%, 0.30%, 0.20%, 0.10%, and 0% NaCl (w/v). After 30 minutes of incubation at room temperature, the mixture was centrifuged at 3,000 rpm for 10 minutes. Each sample was tested in duplicate, and the supernatant was transferred to a spectrophotometer (Eppendorf, MA, USA) for absorbance measurement at 540 nm using 1% NaCl as the blank. The percentage of hemolysis was calculated according to the following formula:

Hemolysis (%): = (OD of test/OD of 0% NaCl) × 100

The effect of commercial paraquat on the osmotic fragility of RBCs in individuals with Hb E trait and G6PD deficiency was assessed as 50% hemolysis or median corpuscular fragility (MCF), respectively. The MCF of normal incubated RBCs ranges from 0.46% to 0.59% NaCl[18,19].

Statistical analysis

The results are presented as the mean ± standard error of the mean (SEM) or the median with range after the normality of data was tested using the Shapiro-Wilk normality test. Statistical analysis was performed with tests appropriate to the dataset, as specified in the figure legends, using GraphPad Prism 10 software (GraphPad, San Diego, CA, USA). A *p*-value of < 0.05 was considered statistically significant.

Results

Screening test for thalassemia, Hb E, and G6PD deficiency

All 18 individuals were screened for thalassemia, Hb E trait, and G6PD deficiency. The results showed that the 10 normal controls were negative for thalassemia according to the OF and DCIP tests, had normal fluorescent spot test results, and their Hb type was A_2A (normal). The four participants with Hb E trait had positive DCIP test results and an EA Hb pattern, whereas they had negative OF test results and normal fluorescent spot test results. The four participants had G6PD deficiency, negative for thalassemia screening and normal Hb type results.

Paraquat induced red blood cell oxidative stress in a concentration-dependent manner

To examine the effect of paraquat on oxidative stress in RBCs, normal RBCs were cocultured with pure (pPQ) and commercially available paraquat (cPQ) at different concentrations for 24 hours. The addition of 200 µg/mL pure paraquat and 100 and 200 µg/mL commercially available paraquat significantly increased the MDA level compared with normal saline in a dose-dependent manner (Figure 1). Moreover, the MDA level in RBCs exposed to 200 µg/mL commercially available paraquat was significantly higher than that of RBCs exposed to other paraquat concentrations (Figure1). These data indicate that paraquat affected RBC lipid membrane peroxidation by inducing oxidative stress.

Increased oxidative stress in red blood cells from participants with Hb E trait and G6PD deficiency

Individuals with Hb E trait and G6PD deficiency are susceptible to oxidative stress; therefore, we investigated the effect of paraquat on oxidative stress in RBCs from participants with Hb E trait and G6PD deficiency. The MDA levels of commercially available paraquat-exposed RBCs from all participants (normal controls and participants with Hb E trait and G6PD deficiency) were significantly higher than the MDA levels of saline-exposed RBCs (Figure 2). Interestingly, the MDA levels of commercially available paraquat-exposed RBCs from participants with Hb E trait were significantly higher than those of RBCs from normal controls, but they were not significantly different from MDA levels of RBCs from participants with G6PD deficiency (Figure 2). These data suggest that RBCs from individuals with Hb E trait are susceptible to paraquat-induced oxidative stress.

Effect of paraquat on erythrocyte osmotic fragility (EOF)

Extensive lipid peroxidation in biological membranes causes fluidity loss, decreased membrane potential, increased permeability to ions, and increased rigidity. To test whether the increase in lipid peroxidation after exposure to paraquat affected RBC membrane rigidity, the EOF of commercially available paraquat-treated RBCs was tested. The results demonstrated that the initial hemolysis of saline- and commercially available paraquat-treated RBCs from individuals with Hb E trait and G6PD deficiency was significantly higher compared with those of normal controls. By contrast, the initial hemolysis (Figure 3A–B) and MCF (Figure 3C) of commercially available paraquat-treated RBCs were not significantly different from those of RBCs from normal controls in all groups. The findings showed that RBCs from individuals with Hb E trait and G6PD deficiency were slightly more fragile than those from normal controls, but paraquat did not affect RBC osmotic fragility.

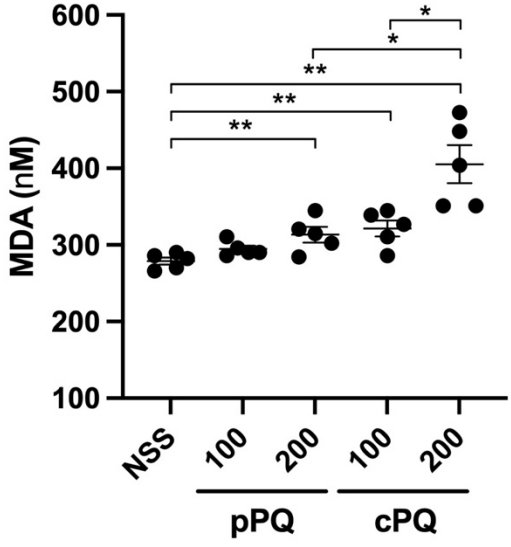

Figure 1 Paraquat induced oxidative stress in RBCs in a concentration-dependent manner.

Note: RBCs of normal controls (n = 5 individuals) were treated with pure paraquat (pPQ) and commercially available paraquat (cPQ). Cell-free supernatants were collected at 24 h and assayed for MDA level by TBARS assay. The results are expressed as mean with standard error of the mean. Statistical significance was determined using paired *t*-test (*p-value < 0.05, **p-value < 0.01).

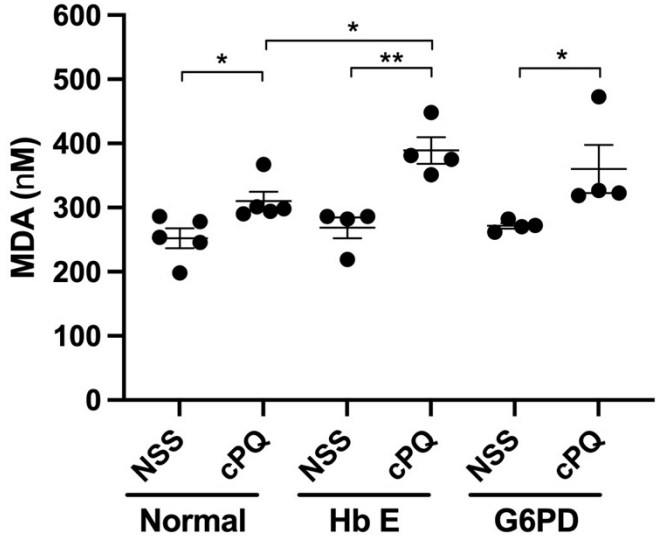

Figure 2 Effect of paraquat on RBC oxidative stress in individuals with Hb E trait and G6PD deficiency.

Note: RBCs of normal controls (n = 5 individuals), individuals with Hb E trait (n = 4 individuals), and individuals with G6PD deficiency (n = 4 individuals) were exposed to 200 µg/mL commercially available paraquat (cPQ) for 24 hours. The results are expressed as median with range. Statistical analysis was performed using the Wilcoxon test or Mann–Whitney U test (*p-value < 0.05, **p-value < 0.01).

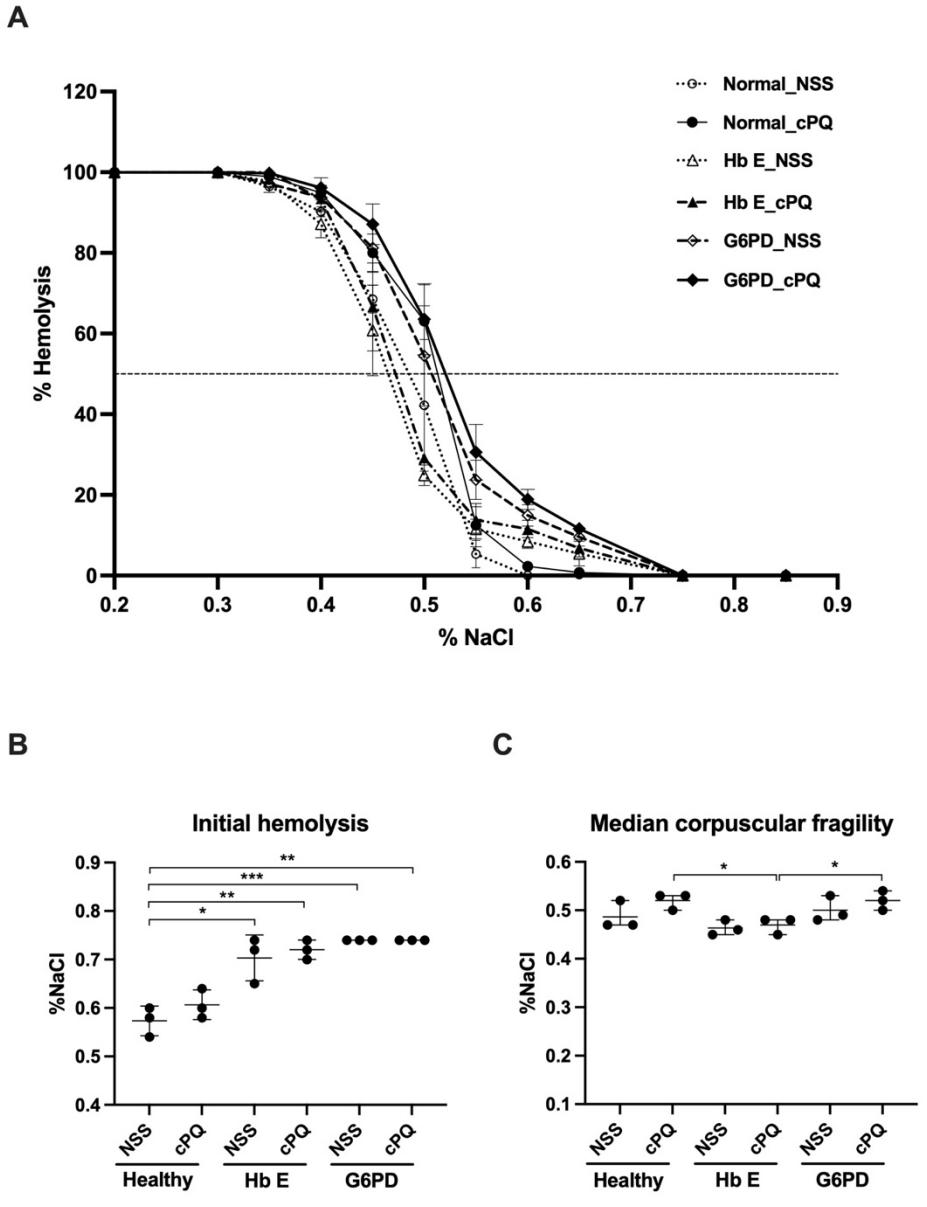

Figure 3 The effect of paraquat on RBC osmotic fragility in individuals with Hb E trait and G6PD deficiency.

Note: RBCs of normal controls and individuals with Hb E trait and G6PD deficiency (n = 3 individuals/group) were exposed to 200 µg/mL commercially available paraquat (cPQ) for 24 hours. A) Erythrocyte osmotic fragility test; B) initial hemolysis; C) median corpuscular fragility. The data are expressed as median with range. Statistical analysis was performed using the Wilcoxon test or Mann–Whitney U test ($^{*}p$-value < 0.05, $^{**}p$-value < 0.01, $^{***}p$-value < 0.005).

Discussion

Paraquat is a potent inducer of intracellular ROS[20-22], which impairs tissue and cell function by inducing lipid peroxidation, protein damage, and DNA breakage[9]. Paraquat induced-oxidative stress affects erythropoiesis in the bone marrow and mature RBCs in circulation, resulting in anemia[7,9]. The present study investigated the effect of paraquat on the lipid peroxidation of the RBCs. The results showed that paraquat significantly increased MDA levels in RBCs after 24 hours in a concentration-dependent manner; similar results have been reported in macrophages and peripheral mononuclear cells[23,24]. Additionally, a previous investigation found that erythrocytes treated with paraquat had higher levels of ROS and lower levels of the superoxide dismutase (SOD) enzyme[9]. Erythrocytes may be more susceptible to ROS and lipid peroxidation because of the decreased SOD levels.

Hemoglobinopathy and G6PD deficiency are common in Thailand. Excessively oxidized globin chains in the RBCs of patients with hemoglobinopathy release free iron, leading to the formation of ROS[25]. In a previous study, higher levels of free radicals resulted in decreased glutathione (GSH) levels and increased lipid peroxidation. Moreover, an ROS-induced decrease in Flippase activity resulted in an increase in phosphatidylserine outer membrane ratios, leading to extravascular macrophage destruction in RBCs[26]. Increased ROS levels cause the oxidation of hemoglobin, lipids, and thiol groups in cytoplasmic membrane proteins. Clusters of oxidized band 3 in the membrane bind immunoglobulin G and complement, causing them to become opsonized and undergo erythrophagocytosis[27]. Intravascular hemolysis occurs in RBCs with more severe damage. RBCs from patients with inherited hemolytic anemia are susceptible to damage from oxidative stress. Our results demonstrated that paraquat was associated with significantly higher levels of lipid peroxidation in RBCs from participants with Hb E trait compared with those from normal individuals. The significantly higher MDA level in Hb E trait RBCs was due to hemoglobinopathy; higher levels of free radicals resulted in decreased GSH levels along with increased lipid peroxidation at baseline. Although MDA levels were higher in participants with G6PD deficiency, the difference was not statistically significant because of the small number of individuals who were G6PD deficient.

The effect of paraquat on RBCs was further investigated with the EOF test. RBCs with damaged membranes had a decreased ability to take in water, leading to hemolysis[18]. The plasma membranes in RBCs are mainly affected by elevated ROS, which cause a variety of problems in the membrane, including lipid peroxidation, protein crosslinking, and protein thiol oxidation[28]. All RBCs treated with paraquat exhibited an increase in osmotic fragility. Paraquat-induced ROS could trigger membrane damage and affect hemolysis resistance at high saline solution concentrations. In individuals with G6PD deficiency, the osmotic fragility curve was shifted to the right. RBCs from patients with G6PD deficiency are unable to produce enough GSH to counteract oxidative stress, which increases membrane damage and causes increased osmotic fragility in G6PD-deficient RBCs compared with RBCs from normal individuals. On the other hand, the osmotic fragility curve for Hb E trait was shifted to the left because RBCs from individuals with Hb E trait have slightly lower MCH levels and a higher surface area to volume ratio[15], they are resistant to osmotic lysis. Therefore, MDA levels and the EOF test results indicated that paraquat induced ROS, which damaged RBC membranes and increased lipid peroxidation. The inability of RBCs from individuals with Hb E trait and G6PD deficiency to respond to oxidative stress results in damage to the RBC membrane and more hemolysis compared with RBCs from normal individuals.

Conclusion

According to the findings of this study, paraquat has a diverse effect on RBCs. Commercially available paraquat concentration of 200 µg/mL induces increased lipid peroxidation in RBCs of individuals with Hb E trait and G6PD deficiency and RBCs of individuals with Hb E trait and G6PD are slightly more fragile than RBCs from normal individuals.

Take home messages

Paraquat induced significantly more oxidative stress and initial hemolysis in RBCs from Hb E trait and G6PD deficiency than normal individuals. This indicates that paraquat residue in food and the environment may damage the RBC membrane and lead to more hemolysis in Hb E trait and G6PD deficiency than in normal individuals.

Conflicts of interest

The authors declare no conflict of interest.

Acknowledgements

This research project was supported by the Thailand Science Research and Innovation Fund and the University of Phayao (Grant No. FF65-UoE011). The Faculty of Allied Health Sciences, Burapha University. The researchers also would like to sincerely thank all subjects for their kind cooperation.

References

1. Pateiro-Moure M, Nóvoa-Muñoz JC, Arias-Estévez M, López-Periago E, Martínez-Carballo E, Simal-Gándara J. Quaternary herbicides retention by the amendment of acid soils with a bentonite-based waste from wineries. J Hazard Mater 2009; 164(2-3): 769-75.
2. Sharma A, Kumar V, Shahzad B, Tanveer M, Sidhu GPS, Handa N, et al. Worldwide pesticide usage and its impacts on ecosystem. SN Appl Sci 2019; 1(11): 1-16.
3. Watts M. Paraquat. [online] 2011 [cited 2023 Jul 27]. Available from: http://wssroc.agron.ntu.edu.tw/note/Paraquat.pdf
4. Gupta S, Garg NK, Shekhawat K. Regulation of Paraquat for wheat crop contamination. Environ Sci Pollut Res 2022; 29(47): 70909-20.
5. Laohaudomchok W, Nankongnab N, Siriruttanapruk S, Klaimala P, Lianchamroon W, Ousap P, et al. Pesticide use in Thailand: Current situation, health risks, and gaps in research and policy. Hum Ecol Risk Assess 2021; 27(5): 1147-69.
6. Prihartono N, Kriebel D, Woskie S, Thetkhathuek A, Sripaung N, Padungtod C, et al. Risk of aplastic anemia and pesticide and other chemical exposures. Asia-Pacific J Public Heal 2011; 23(3): 369-77.
7. Bhardwaj N, Singh A. Paraquat treatment modulates integrin associated protein (CD47) and basigin (CD147) expression and mitochondrial potential on erythroid cells in mice. Environ Toxicol Pharmacol 2018; 58: 37-44.
8. Ciccoli L, De Felice C, Paccagnini E, Leoncini S, Pecorelli A, Signorini C, et al. Erythrocyte shape abnormalities, membrane oxidative damage, and ß-actin alterations: An unrecognized triad in classical autism. Mediators Inflamm 2013; 2013: 432616
9. Bhardwaj N, Saxena RK. Elimination of young erythrocytes from blood circulation and altered erythropoietic patterns during paraquat induced anemic phase in mice. PLoS One 2014; 9(6): e99364.
10. Kittisares K, Palasuwan D, Noulsri E, Palasuwan A. Thalassemia trait and G6PD deficiency in Thai blood donors. Transfus Apher Sci 2019; 58(2): 201-6.
11. Nanakorn N, Chuechan S. Impaired oxidative stress in Thalassemia-Hemoglobin E traits after acute exhaustive exercise. Sport Sci Health 2022; 18(3): 789-97.

12. Palasuwan A, Soogarun S, Wiwanitkit V, Luechapudiporn R, Pradniwat P, Lertlum T. Preliminary study of the effect of vitamin E supplementation on the antioxidant status of hemoglobin-E carriers. Southeast Asian J Trop Med Public Health 2006; 37: 184-9.
13. Palasuwan A, Soogarun S, Suksom D, Pitaksathienkul C, Rousseau AS. Antioxidant status in hemoglobin E carriers after acute and chronic strenuous exercises. Res Sport Med 2015; 23(4): 351-66.
14. Karadsheh NS, Quttaineh NA, Karadsheh SN, El-Khateeb M. Effect of combined G6PD deficiency and diabetes on protein oxidation and lipid peroxidation. BMC Endocr Disord 2021; 21: 246.
15. Fucharoen G, Sanchaisuriya K, Sae-Ung N, Dangwibul S, Fucharoen S. A simplified screening strategy for thalassaemia and haemoglobin E in rural communities in south-east Asia. Bull World Health Organ 2004; 82(5): 364-72.
16. Prakobkaew N, Buddhisa S. The prevalence of glucose-6-phosphate dehydrogenase deficiency in Trat province, eastern Thailand. Arch Allied Heal Sci 2022; 34(2): 35-43.
17. Klarod K, Singsanan S, Thamwiriyasati N, Ladawan S, Luangpon N, Boonsiri P, et al. Effects of Qigong exercise on muscle strengths and oxidative stress/antioxidant responses in young sedentary females: a quasi-experimental study. J Exerc Rehabil 2020; 16(5): 418-26.
18. Layton M, Roper D. Investigation of the Hereditary Haemolytic Anaemias: Membrane and Enzyme Abnormalities. 12th ed. Dacie and Lewis Practical Haematology. Elsevier Ltd.; 2017.
19. Jaroonwitchawan T, Chaicharoenaudomrung N, Namkaew J, Noisa P. Curcumin attenuates paraquat-induced cell death in human neuroblastoma cells through modulating oxidative stress and autophagy. Neurosci Lett 2017; 636: 40-7.
20. Drechsel DA, Patel M. Chapter 21 Paraquat-Induced Production of Reactive Oxygen Species in Brain Mitochondria. Methods in Enzymology. Methods Enzymol 2009; 456: 381-93.
21. Wang X, Luo F, Zhao H. Paraquat-induced reactive oxygen species inhibit neutrophil apoptosis via a p38 MAPK/NF-κB-IL-6/TNF-α positive-feedback circuit. PLoS One 2014; 9(4): 1-7.
22. Valko M, Leibfritz D, Moncol J, Cronin MTD, Mazur M, Telser J. Free radicals and antioxidants in normal physiological functions and human disease. Int J Biochem Cell Biol 2007; 39(1): 44-84.
23. Kim H, Lee SW, Baek KM, Park JS, Min JH. Continuous hypoxia attenuates paraquat-induced cytotoxicity in the human A549 lung carcinoma cell line. Exp Mol Med 2011; 43(9): 494-500.
24. Huang J, Ning N, Zhang W. Effects of paraquat on IL-6 and TNF-α in macrophages. Exp Ther Med 2018; 1783-9.
25. Fibach E, Rachmilewitz E. The Role of Oxidative Stress in Hemolytic Anemia. Curr Mol Med 2008; 8(7): 609-19.
26. Mohanty JG, Nagababu E, Rifkind JM. Red blood cell oxidative stress impairs oxygen delivery and induces red blood cell aging. Front Physiol 2014; 5: 1-6.
27. Luzzatto L, Ally M, Notaro R. Glucose-6-phosphate dehydrogenase deficiency. Blood 2021; 136(11): 1225-40.
28. Fibach E, Dana M. Oxidative Stress in β-Thalassemia. Mol Diagnosis Ther 2019; 23(2): 245-61.

Arch AHS

ORIGINAL ARTICLE

Archives of Allied Health Sciences 2023; 35(3): 48-53.

Did digital learning during the lockdown impact emotional distress?

Supalak Khemthong, Maliwan Rueankam, Winai Chatthong*

Department of Occupational Therapy, Faculty of Physical Therapy, Mahidol University, Nakhon Pathom, Thailand.

KEYWORDS
Sleep health;
Emotional health;
Occupational therapy;
Digital learning.

ABSTRACT

Digital learning might have been one helpful strategy for occupational therapy students during the coronavirus pandemic in 2019. This study aimed to assess, before and after the lockdowns, whether digital learning caused any changes or had any impact in terms of the sleep quality, sleep hygiene, and emotional distress experienced by the 1st – 3rd year students during two semesters between 2020 and 2021. The Thai version of the Pittsburgh Sleep Quality Index, Sleep Hygiene Index, and Depression Anxiety Stress Scales were assessed in purposive sampling of 42 students. It was found that sleep hygiene and quality were not significantly different, while depression, anxiety, and stress scores increased significantly in 2021. Even though all students were able to maintain grade point averages, they perceived poor sleep quality and moderate sleep hygiene after the 9-month lockdown. This study suggests that coping strategies with resiliency, mental health well-being, and sleep health management might be an integrated topic for digital learning. In conclusion, the lockdown situation has cultivated a significant uptrend in emotional distress without differences in academic success among the participants.

***Corresponding author:** Winai Chatthong, PhD, OTR. Faculty of Physical Therapy, Division of Occupational Therapy, Mahidol University, Nakhon Pathom, Thailand. Email address: winai.cha@mahidol.edu
Received: 26 July 2023/ Revised: 10 October 2023/ Accepted: 17 November 2023

Introduction

University lecturers adopted online teaching during the coronavirus pandemic or COVID-19. Hours of planning, preparation, and reflection in breakout rooms were required for occupational therapy students (OTS). New learning skills were developed such as telehealth, simulated clients as well as experiencing different sessions with exhaustion throughout the day[1]. Some occupational therapy educators are enthusiastic facilitators in terms of delivering quality instruction with encouragement for sharing professional experiences[2]. However, online teaching requires time-consuming course preparation. It is challenging to use video simulations of clients that allow the OTS to make essential decisions similar to the real demands for professional health education[1,2]. Currently, online teaching mixed with various types of digital learning (e.g., flipped, blended, hybrid, e-learning) has been reported to be equivalent to or more effective than traditional face-to-face (F2F) classroom instruction among the OTS[3].

The new everyday phenomena of smartphones and internet users have also developed the need for multipurpose digital learning[4]. However, the 1st – 4th year OTS (n = 110) in India who had internet addiction (57.28%) perceived poor quality of sleep (75%) in moderate correlation with high levels of stress (14.54%)[5]. This is similar to the first-to-fourth-year OTS in South Africa (n = 117), who were found to be highly affected by academic stress-related health science and clinical education[6]. OTS might have been coping with overloaded online schedules, especially for some dependent and unorganized students[2] or those with poor coping strategies for resilience (e.g., disorganized adaptability and psychological insecurity)[7,8].

Moreover, the first-to-fourth-year OTS in a university in Thailand (n = 52) perceived poor quality of sleep to be moderately correlated with emotional distress during COVID-19[9]. The unwell sleep OTS (n = 30) gained higher comorbidities of smartphone, internet addiction, and emotional states than those well sleep OTS (n = 22) in the academic year 2020. Sharma, Tyszka[10] found that American OTS (n = 332) perceived emotional distress, i.e. depression (52.4%), anxiety (62.6%), and stress (87.7%) during COVID-19 in the academic year 2021. Also, they reported that the lockdown situation decreased social participation and reduced physical leisure activities, leading to intense, pervasive negative feelings of sadness and depression[10].

A further determination is required for the OTS on whether there was a change before and after the 9-month lockdown, in other words, a transition between the academic years of 2020 and 2021. Therefore, this study was interested in comparing the sleep and emotional distress parameters among the first-to-third-year OTS at a university in Thailand during the 9-month lockdown and digital learning due to COVID-19.

Materials and methods

Participants and procedure

This study was a causality with the before-and-after (twice data collection) lockdown situation and digital learning between two academic years (9 months) during the COVID-19 pandemic. Purposive sampling was used by inviting the OTS, 1st to 3rd years at one university during the academic year 2021, who had engaged in a previous study (n = 42)[9] to receive follow-up over a period of 9 months.

Sample size and subject selection

Data from a previous study by the authors in the 1st to 4th OTS for academic year 2020 (n = 52)[9] and the results of the American OTS[10] the Depression Anxiety Stress Scale (DASS-21) averaged scores of depression and its cut-off scores provided in the DASS manual[11] were used to calculate by G*Power software (version 3.1.9.4) with 2.02 of critical t-test. The data indicated that this study required at least 40 samples, at the 80% power of effect size. To minimize the risk of miscalculation, a replacement participant could be accepted in the event of a withdrawal by a participant.

To prevent biopsychosocial confounding factors, the inclusion criteria for subject selection included having no history of physical or neuropsychiatric disorders. To ensure the absence of a pertinent history concerning any disorders, all participants were asked to answer two yes/no questions in the online survey concerning medical diagnoses and use of medications in the past to the present, including physical activity routines during the COVID-19 pandemic.

Instruments for data collection

The online survey consisted of five sections comprising the following standardized instruments: the Thai version of the Pittsburgh Sleep Quality Index (T-PSQI), the Sleep Hygiene Index: Thai version (SHI: Thai version), and the DASS-21: Thai version. Demographic information was also collected, including birthdate, gender, and grade point average (GPA).

The T-PSQ[12] was used to assess overall sleep quality over one month and consisted of 19 self-rated items. Each item was scored from 0 (no difficulty) to 3 (severe difficulty). An overall score of less than or equal to 5 indicated good sleep quality. Its psychometric properties were previously reported to possess acceptable internal consistency and reliability (α = 0.73) as well as a sensitivity tool of 89.6% for sleep quality assessment[12]. This study considered a cut-off score above 5 to indicate poor sleep quality[12].

The Thai version of the SHI has previously been addressed as having acceptable internal consistency and reliability (α = 0.73)[13]. It consists of 14 questions for sleep hygiene behaviors; scores ranged from "5", indicating the most practiced behavior, to "1", indicating the least practiced behavior. A low level of practice in terms of sleep hygiene behaviors scored 1.00-2.33, while a moderate level scored 2.34-3.66, and a high level scored 3.67-5.00[13]. This study considered a cut-off score below 3.67 to indicate poor sleep hygiene[13].

The Thai version of the DASS-21 consists of 21 questions on emotional states with a previous report for acceptable to good internal consistency and reliability[14]. The scoring criterion for each item was between 0 and 3, which needed to be multiplied by 2 to gain the final score for each level[11,14]. This study considered cut-off scores below 10, 8, and 15 for normal levels of emotional states or without depression, anxiety, and stress, respectively[11]. Raw data per participant of score interpretation was counted of 5 levels for each emotional state (depression, anxiety, and stress) i.e., normal, mild, moderate, severe, and extremely severe. and then all counted scores were calculated as percentages for all participants.

Statistical analysis

All obtained data were analyzed using the IBM Statistical Package for the Social Sciences (IBM SPSS) version 2. Descriptive statistics were used to explain the data. Also, paired-samples t-tests were calculated at a *p*-value threshold of 0.05.

Results

Sample characteristics

During the nine-month data collection, a total of 42 OTS were recruited; most of them were females (n = 35). In the raw data, there were only 7.14% vs. 14.29% of OTS who received GPAs less than 3.00 in the year 2020 vs. 2021, respectively. Interestingly, the OTS were able to improve their GPA by around 40.48% during a period of nine months (no change 38.09%; decrease 21.43%). A paired-samples t-test showed no significant difference in ages as converted from birthdates and GPA (Table 1).

Sleep quality and hygiene

A paired-samples t-test found no significant difference between the post- versus pre-scores of the T-PSQI and the SHI. The raw data of OTS were 59.52% poor quality of sleep and 73.81% moderate sleep hygiene in the year 2021, whereas 54.76%

poor quality of sleep and 76.19% moderate sleep hygiene were shown in 2020. During a period of nine months, there was continuing moderate sleep hygiene (positively changed by 2.38%), but the OTS had negatively changed sleep quality by around 4.76%.

Table 1 Personal data and outcomes of the study

Variables	Year 2020 (n = 42)	Year 2021 (n = 42)	*p*-value*
Age (years)	19.33 ± 0.85	19.38 + 0.79	1.60
GPA	3.29 + 0.39	3.40 + 0.38	0.25
T-PSQI	6.12 ± 2.28	6.45 ± 3.10	0.59
SHI	3.51 ± 0.36	3.51 ± 0.33	0.99
DASS-21			
Depression	4.52 ± 3.00	12.90 ± 7.10	< 0.001
Anxiety	4.38 ± 3.13	9.48 ± 6.03	< 0.001
Stress	3.33 ± 2.24	11.24 ± 8.04	< 0.001

Note: The data were reported using mean ± standard deviation. *The data were compared using the paired-samples t-test.

Abbreviations: GPA, grade point average; T-PSQI, Thai version of the Pittsburgh Sleep Quality Index; SHI, Sleep Hygiene Index-Thai version; DASS-21, Depression Anxiety Stress Scale-Thai version.

Emotional states

There was a significantly higher score for depression compared to the previous year's scores. The OTS did have significantly higher anxiety compared to the last year's score for anxiety. The raw data for OTS revealed 64.29% (1 extremely severe, 4 severe, 16 moderates, and 6 mild depression) in the year 2021, whereas there were only 11.90% (5 mild depression)—in 2020. Later, there were 30.95% (1 extremely severe, 2 severe, 5 moderate and 5 mild of anxiety) in the year 2021 whereas there were 26.19% (6 moderate and 5 mild anxiety) in 2020. None of the former OTS were found to be stressed, but the later OTS were found to include 30.95% (1 extremely severe, 2 severe, 5 moderate and 5 mild stress). Only 11.90% of the OTS had positively changed depression levels in both years (no change 9.52% and negative change 78.58%).

Discussion

This study found no significant differences in age, GPA, sleep quality or hygiene for the OTS in both years. As seen in the scoring interpretation, the OTS remained having poor sleep quality and moderate sleep hygiene for a period of nine months. All three types of emotional distress were significantly shown to have higher scores in the year 2021, with mild to extreme levels of depression, anxiety, and stress. In contrast to the year 2020, the OTS gained mild depression and anxiety, whereas normal stress was addressed.

Interestingly, the OTS perceived an interesting benefit of digital learning that the emotional distress accompanied with the trend of improved GPA of those participants (40.48%). As seen in table 1, their means have changed from 3.29 to 3.40 with the similar range of SD. Using digital learning might be a good life experience due to personal and social adaptability during

the period of the 9-month lockdown, similar to the study of Brown et al[7], who mentioned that OTS could have perceived stress as being associated with self-control and a positive outlook. Our educators have supported the OTS for developing their competencies[1] (e.g., self-regulation skills for time management) and protective factors[6] (e.g., social supportive circumstances and resilience behavior). Importantly, most OTS were able to achieve academic improvement during the lockdown, meaning they could utilize the effective design of digital learning, similar to a previous study[3]. However, the current study found mild to extreme stress in 2021 indicating that academic stress might be one confounding factor for individual levels of listening skills in the context of online classrooms[7] (e.g., data downloading, active listening, and empathetic listening toward proactive instructors).

It has been accepted[7,9] that poor sleep OTS (poor sleep quality and moderate sleep hygiene) were not spending long hours of digital learning, but they perceived mild smartphone and internet addiction for family/peer contacts at nighttime in correlation with mild emotional distress. The current study found non-significant differences in sleep parameters which may imply their poor sleep behavior prior to the lockdown period, and it was remained as usual behavior throughout the period of data collection. Consequently, the poor sleep OTS could not avoid emotional distress and have delayed internet access at home[1] during COVID-19 because a turning point of accumulative stress episodes might increase in symptoms of depression and anxiety in 2021. Those participants may have been feeling of sadness (reduced social participation) and loneliness (low motivation toward increased social isolation) as described in the previous studies under an unsafe/unhealthy context[9,10]. This statement indicates that personal coping strategies of resilience might be a medium to decrease the risk of health behavior as seen from a minor improvement in sleep hygiene in 2021.

Study limitations and recommendations for future studies

This study could not identify a cause or effect of the lockdown situation separately from digital learning. Further studies should consider the use of a controlled study mixed with a qualitative study on any confounding and protective factors related to mental health well-being and academic success.

Conclusion

This study highlights a significant uptrend in terms of depression, anxiety, and stress after nine months of lockdown and digital learning experienced by OTS at a university in Thailand.

Clinical implications

- There was no impact on GPA, sleep quality, and sleep hygiene during the period of nine-month lockdown and digital learning although the OTS perceived emotional distress.
- Poor sleep quality and moderate sleep hygiene might be personal variation due to emotional distress under unsafe circumstances.
- The significant worsening of emotional state of the OTS might be a warning sign to support and monitor before two academic years of lockdown situation.

Conflicts of interest

The authors declare no conflicts of interest in the completion of this work.

Acknowledgements

The authors would like to thank the Faculty of Physical Therapy for its support and the undergraduate students of the occupational therapy program for their participation.

References

1. Gustafsson L. Occupational therapy has gone online: What will remain beyond COVID-19? Aust Occup Ther J 2020; 67(3): 197-8.
2. Hollis V, Madill H. Online learning: the potential for occupational therapy education. Occup Ther Int 2006; 13(2): 61-78.
3. Hwang NK, Shim SH, Cheon HW. Digital learning designs in occupational therapy education: a scoping review. BMC Med Educ 2023; 23(1): 7.
4. Park CS. Examination of smartphone dependence: functionally and existentially dependent behavior on the smartphone. Comput Hum Behav 2019; 93:123-8.
5. Shitole BS, Jitta SP, Netikar HM, Panchasara TP. Identifying internet addiction, quality of sleep and stress among undergraduate (UG) occupational therapy (OT) students: a cross sectional study. Indian J Appl Res 2020; 10(4): 84-6.
6. De Witt P, Monareng L, Abraham A, Koor S, Saber R. Resilience in occupational therapy students. S Afr J Occup Ther 2019; 49(2): 33-41.
7. Brown T, Yu M-l, Etherington J. Listening and interpersonal communication skills as predictors of resilience in occupational therapy students: a cross-sectional study. Br J Occup Ther 2021; 84(1): 42-53.
8. Geirdal AO, Nerdrum P, Bonsaksen T. The transition from university to work: what happens to mental health? a longitudinal study. BMC Psychol 2019; 7(1): 1-10.
9. Chatthong W, Khemthong S, Rueankam M. Relationship between sleep, digital usage and emotional states in Thai occupational therapy students. Asia Pac J Health Manag 2021; 16(4): 116-24.
10. Sharma A, Tyszka A. Understanding the mental health of occupational therapy students during the COVID-19 pandemic. J Occup Ther Edu 2023; 7(1).
11. Lovibond SH, Lovibond PF. Manual for the depression anxiety stress scales. 2nd ed. Sydney: Psychology Foundation; 1995.
12. Sitasuwan T, Bussaratid S, Ruttanaumpawan P, Chotinaiwattarakul W. Reliability and validity of the Thai version of the Pittsburgh sleep quality index. J Med Assoc Thai 2014; 97 (Suppl 3): S57-67.
13. Mairs L, Mullan B. Self-monitoring vs. implementation intentions: a comparison of behaviour change techniques to improve sleep hygiene and sleep outcomes in students. Int J Behav Med 2015; 22(5): 635-44.
14. Oei TPS, Sawang S, Goh YW, Mukhtar F. Using the depression anxiety stress scale 21 (DASS-21) across cultures 2013; 48(6): 1018-29.